Coordination Chemistry Reviews 254 (2010) 2429–2445

Contents lists available at ScienceDirect

Coordination Chemistry Reviews

journal homepage: www.elsevier.com/locate/ccr

Review

Harnessing supramolecular interactions in organic solid-state devices: Current status and future potential

Dario M. Bassani*, Laura Jonusauskaite, Aurélie Lavie-Cambot, Nathan D. McClenaghan*, Jean-Luc Pozzo*, Debdas Ray, Guillaume Vives

Institut des Sciences Moléculaires, CNRS/Université Bordeaux 1, 351 cours de la Libération, 33405 Talence, France

Contents

ARTICLE INFO

Article history:
Received 7 February 2010
Accepted 15 May 2010
Available online 31 May 2010

Keywords:
Supramolecular chemistry
Devices
Organic photovoltaics
OLED
OFET
Molecular logic

ABSTRACT

The performance attained by electronic devices incorporating more than a single molecule is in part limited by weak electronic coupling between molecules. By implementing designed supramolecular interactions, chemists have begun taking control of the nanoscale ordering of the active layer in an effort to move beyond the trial and error tuning of the device morphology. This review describes current progress in solid-state devices in which the molecular components possess designed supramolecular interactions – as opposed to non-specific cohesive forces – used to instill or modify functionality. Supramolecular organic devices for applications in solar energy conversion, light-emitting diodes, field-effect transistors, storage and logic functions are covered.

1. Introduction

Interest in organic materials for applications in electronics was launched by Aviram and Ratner's seminal 1974 article on the propensity of a single molecule to act as a rectifier circuit [1]. Since then, this and other theoretical predictions (quantized conductance, dephasing, Coulomb blockade) have been experimentally documented despite the great difficulties inherent to single-molecule experiments. While integrated circuits based on single-molecule components may one day emerge [2–12], it is much more likely that initial devices will contain a non-discrete number of molecules cast into the active area of the component. Although the allure of miniaturization beyond silicon is lost, such components are much easier to manufacture than single-molecule devices and remain appealing in view of the unique properties of molecules *vs.* semiconductors, which include transparency in the visible region of the spectrum, flexibility, and potential for facile low-cost fabrication.

It is interesting to remark that the same forces that make molecules appealing are at the heart of their shortcomings. The well-defined electron density map that characterizes a molecule determines its relatively narrow electronic absorption spectra, but also signifies that intermolecular electronic overlap integrals are small except in specific cases, e.g. when π-stacking is important. One fortunate outcome of this is that molecule-based electronic materials are much less susceptible to defects and impurities, as their effect is localized to nearby molecules only. However, this lack of intermolecular electronic communication abates the

* Corresponding authors. Tel.: +33 540002827/3321/2752.
E-mail addresses: d.bassani@ism.u-bordeaux1.fr (D.M. Bassani), n.mc-clenaghan@ism.u-bordeaux1.fr (N.D. McClenaghan), jl.pozzo@ism.u-bordeaux1.fr (J.-L. Pozzo).

0010-8545/$ – see front matter © 2010 Elsevier B.V. All rights reserved.
doi:10.1016/j.ccr.2010.05.007

charge-carrier mobility, which ultimately clamps device performance. The introduction of long-range order can restore high charge-carrier mobility, for example in crystalline samples, but this would be detrimental for the flexibility of the device, which benefits from amorphous materials, and potentially costly to manufacture.

What then, is the solution to improve the properties of molecular materials for organic electronic applications? How can one introduce long-range order without compromising flexibility and ease of manufacture? The problem is an old one, which involves up-scaling order from the molecular level to – at least – the nano- or microscopic domain. As it turns out, a possible solution to this conundrum is also equally old, and has been used by Nature for millennia: supramolecular self-assembly. Using this, Nature builds molecular components that spontaneously self-assemble into ordered architectures with designed functionalities. By controlling the type and number of interactions, it is possible to obtain very precise architectures (e.g. the photosynthetic reaction center in bacteria), or more flexible systems that are tolerant of physical deformations, such as cellular lipid bilayer membranes.

The underlying principle behind the use of designed intermolecular interactions in organic electronic devices is to dissociate the fundamental electronic properties of the molecular component (principally determined by its electronic structure) from its self-aggregation properties which drive the morphology of the molecular active layer of the device. The latter is important in controlling through-space interactions which in turn determine long-range charge transport. Since device performance is to a large extent determined by the mobility of charge carriers, independent control of the morphology and electronic properties will in principle allow one to separately tune electronic characteristics while optimizing charge transport. Materials capable of self-assembly are of interest here, since they have the potential to form well-defined structures in which molecular ordering facilitates efficient charge transport. The quality of the intermolecular interaction (in terms of the magnitude of the charge-transfer integral between adjacent sites) is of course dependant on the relative orientation and distance of the molecular components. Depending on the degree of order within the material, different theoretical models can be used to describe the mobility of charge carriers, from band theory for structurally ordered materials, to tight-binding models for weakly disordered systems, and hopping models for localized charges in strongly disordered materials. An overview of charge-transport models applicable to self-organizing molecular materials is provided by Grozema and Siebbels [13].

Numerous examples attest to the importance of the effect of molecular order on charge-carrier mobility. The charge-carrier mobility of α-sexithiophene, for example, has improved from 10^{-4} $cm^2/V s$ in early measurements on amorphous films to 0.1 $cm^2/V s$ in the crystalline phase [14]. Liquid-crystalline materials offer the unique opportunity to follow the electronic properties of a device as a function of molecular order by varying the temperature over a narrow range centered on a phase transition in the material. For example, charge-carrier mobilities as high as 1 $cm^2/V s$ were found (by time-resolved microwave conductivity measurements) for a hexabenzocoronene discotic liquid-crystalline material when in the crystalline phase which, upon heating to a temperature above the $K_2 \rightarrow D_h$ transition (*ca.* 100 °C), undergoes a sudden 4-fold drop in charge-carrier mobility [15]. In another case, the degree of order in the columnar packing of triphenylene liquid-crystalline materials was improved by the introduction of secondary amide groups capable of hydrogen-bonding interactions linearly aligned to the direction of the columnar stacks, resulting in a charge-carrier mobility that is *ca.* five times higher than for conventional triphenylene-based liquid-crystalline materials [16]. The applicability of discotic liquid crystals for organic electronics has been recently reviewed several times [17–24] and will not be further discussed herein, except for selected examples involving illustrative cases of supramolecular interactions.

Supramolecular interactions loosely cover a wide range of intermolecular forces, ranging from hydrophobic/dispersion forces, to hydrogen-bonding (H-B) and metal ion coordination. The forces generated by these interactions also span a wide gamut, from <1–4 kJ/mol for the relatively weak hydrophobic, aromatic π-stacking interactions and single-point H-B, to >250 kJ/mol for very strong coordinative bonds. Besides the free energy, other factors such as kinetic lability and directionality also describe supramolecular interactions. Thus, some (e.g. H-B and coordination bonds) are directional, others only partly directional (e.g. π-stacking), while others are non-directional (dispersive forces). Clearly, directionality is desirable in cases where a bottom-up design is expected to lead to the formation of precise, well-defined architectures. For these applications, the use of H-B and coordinative bonds has been privileged, with H-B interactions being particularly well-suited towards the construction of photoactive supramolecular assemblies [25,26]. Aromatic π-stacking, a principal driving force behind the formation of discotic liquid crystals, also ensures moderate to good electronic communication between the electron clouds of the molecular components [20]. When the electronic interactions are sufficiently strong or driven by external forces [19], the formation of *J*- or *H*-type aggregate structure and their subsequent effect on the electronic absorption and emission spectra is observed.

Supramolecular chemistry thus offers a promising route to bridge the gap between the single-molecule world and real-life nano- to micron-scale devices, allying the advantages of molecular design (synthesis, purification, and characterization) and the advantages of solution-based processing (low cost, easy up-scaling). Further down the line, behaviour specific to dynamic supramolecular components may also be harnessed, such as autonomic regulation and self-healing [27–30]. Despite this, the number of examples involving molecule-based devices in which designed supramolecular self-assembly is used remains relatively limited. The two-fold reason for this is that (1) it is still difficult to relate molecular structure to supramolecular self-assembly in the solid, particularly for multifunctional molecules where more than one interaction is present (e.g. π-stacking by an aromatic core, hydrophobic forces from solubilizing side-chains, and H-B groups for self-assembly); and (2) design principles relating the morphology of the active layer to the performance of organic devices are poorly understood. Additionally, fine-tuning of the solubility *vs.* aggregation properties is required to obtain materials that spontaneously self-assemble in the solid while maintaining good processability from solution.

In the following pages, a review of current systems in which designed supramolecular interactions (as opposed to non-specific aggregation) are used in the manufacture of the active layer in organic electronic devices is presented. Emphasis is placed, as far as possible, on those systems that actually led to a physical solid-state device, and not towards more common solution-based systems. The former are sub-divided according to application, which focus on supramolecular materials for organic light-emitting diode (OLED), organic photovoltaic (OPV), and organic field-effect transistor (OFET) devices, as well as supramolecular materials for storage and logic. It is hoped that this compilation will assist the field in honing design principles relating molecular structure to the self-assembly and electronic properties of the active layer in organic devices.

2. Supramolecular materials for organic field-effect transistors

Organic field-effect transistor (OFET) devices [31] have attracted significant attention because of their potential use as soft channel

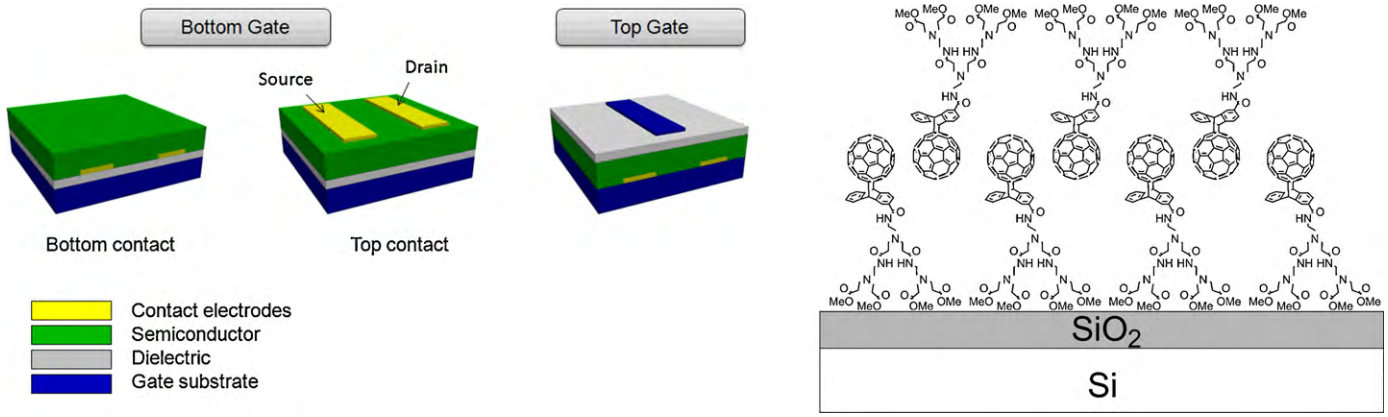

Fig. 1. *Left*: Common fabrication architectures for OFET devices. *Right*: Schematic representation of the fullerodendron assemblies in the active layer of OFET devices reported by Kusai et al. [55].

materials in organic/printed optoelectronic devices such as active-matrix flat-panel displays (AMFPDs), electronic paper, RF-ID tags, and chemical/biosensors [32–39]. The detailed basis of OFET operation has been reported in a number of reviews [40–46]. Briefly, OFETs require a thin organic semiconductor layer separated from a gate electrode by an insulating gate dielectric. The semiconducting layer is in contact with source and drain electrodes of channel width *W* separated by a channel length *L*. Fig. 1 depicts the common device configurations used in OFETs, which can be either bottom-gate or top-gate. In the first configuration, two different structures can be used, bottom-contact or top-contact, depending on the position of the drain and source electrodes. Each construction possesses its own advantages: for a top contact-bottom gate (TC/BG) device geometry, contact resistance is minimal and the charge mobilities tend to be higher. However, it is still a challenging task to downsize the channel dimensions which are usually >5 μm. For the bottom contact geometry, the difficulty in preparing highly ordered films on irregular surfaces is a limiting parameter to the overall device performance. Nonetheless, these devices are more easily prepared and integrated into low-cost manufacturing processes and, compared to TC/BG devices, smaller sizes can be obtained.

It is accepted that the local structure of the organic semiconductor plays a key role in determining the OFET performance [42]. In addition to stability and energetic considerations, the orientation of the molecules to each other and the associated electron transfer integrals are of paramount importance [47]. Most polymeric or oligomeric systems tend to form ordered regions of typically 200–300 nm in size, which is much smaller than the dimensions of typical micrometre-scale devices. A common problem is that OFETs tend to suffer from electrical instability under external bias arising from charge traps created by the appearance of disorder-induced defects. The crucial process of charge accumulation and transport under an external field taking place very close to the interface between the gate dielectric and the semiconductor is the principal factor controlling the electronic characteristics of the device [48]. In this regard, ordering organic solid-state π-conjugated materials by employing non-covalent interactions, including Coulombic, van der Waals or hydrophobic forces, π–π stacking, or hydrogen bonding, is particularly relevant for improving the properties of the resulting OFET devices. Different approaches using secondary interactions are illustrated below.

The ability of π-conjugated systems to self-assemble *via* π–π stacking [49,50] has been fruitfully exploited for preparing a wide range of highly ordered architectures which have found various applications in microelectronics [51–53]. In the case of oligomers and polymers, the semiconducting layer is usually spin-coated or drop cast, whereas small organic molecules are usually deposited *via* vacuum sublimation, which additionally results in very high chemical purity of the sample. More recently, a solution-shearing process has been developed that leads to large crystalline domains based on the π-stacking of quaterthiophene motifs possessing an elongated shape along the shearing direction [54]. Various geometries can be obtained according the conditions and the shearing speed. Kusai et al. have designed fullerodendrons as good semiconductor candidates to develop solution-processed FET devices [55]. The highly dense and functional terminal groups of dendron facilitate the formation ordered structures, which mainly rely on π-stacking to afford supramolecular structures possessing efficient π-orbital overlap between the C_{60} moieties (Fig. 1).

Recently, Bao and co-workers designed a liquid-crystalline semiconducting polymer by combining an electron-donating quaterthiophene with electron-accepting bithiazole units. The resulting liquid-crystalline film maintains self-organization due to strong intermolecular interactions, and adopts a well-ordered π–π stacking architecture that is parallel to the substrate surface [56]. A related approach to ensure a long-range connectivity among semiconducting moieties relies on the use of self-assembled monolayers (SAMs). However, an optimized and near-perfect coverage must be attained in order to reach high current densities [57–59]. The self-assembly of pentathiophene derivatives which serve as an organic semiconductor is responsible for the conducting path between the source and drain electrodes [60]. Copolymers incorporating naphthalene-1,4,5,8-bis(dicarboximide) (NDI) and bithiophene units have been designed to ensure a strong electron-depleted structure [61]. The NDI motif was chosen for its excellent electronic properties but also because it induces the formation of a regioregular and highly π-conjugated polymeric backbone [62].

One-dimensional organic semiconductor nanostructures such as nanowires and nanobelts offer interesting features to control the semiconductor structure. Such nanobelt architectures were recently prepared from poly(benzobisimidazobenzophenanthroline) polymers which exhibit *n*-channel transport properties even in the presence of oxygen [63]. The very rigid and planar molecular backbone enables the polymer chains to form intermolecular π–π stacking, calculated to be as strong as 160 kJ/mol, which governs the self-assembly process and consequently induces enhanced charge-carrier mobility. On another hand, Heath et al. employed the superlattice nanowire pattern technique to construct 2D nanowire structures templated on a single crystal substrate at sublithographic dimensions, where van der Waals interactions play a key role in the formation of ultradense arrays of the aligned and closely spaced nanowires [64]. Printing techniques constitute a promising approach for low-cost and large-area manufacturing of electronics. Major drawbacks typically

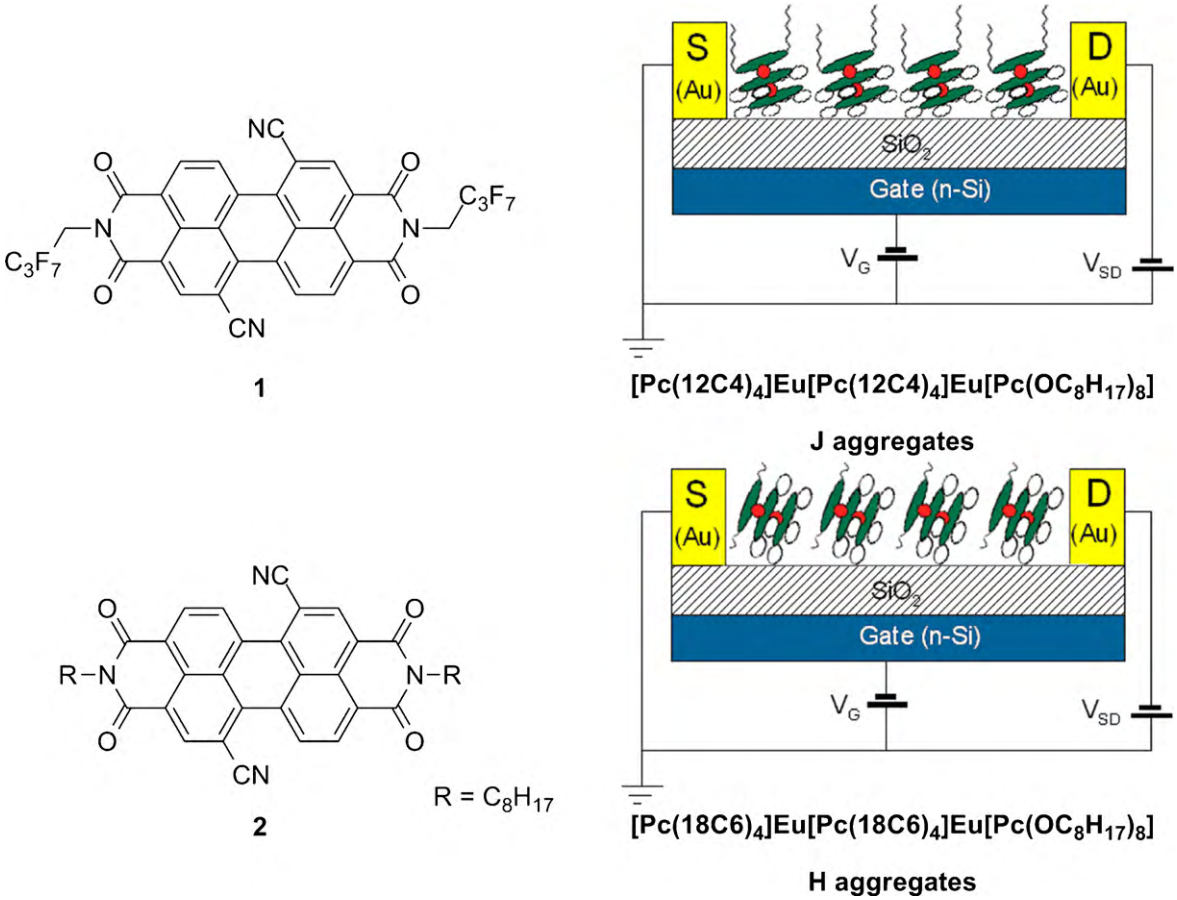

Fig. 2. Fluorination of the hydrocarbon chains in perylene alkyldiiimide derivatives (compounds **1** and **2**) was found to favor face-to-face arrangements of the aromatic cores, thereby resulting in a 10-fold enhancement of the observed charge-carrier mobility in OFET devices. *Right*: Schematic arrangement of heteroleptic tris(phthalocyaninato) europium complexes reported by Gao et al. [68]. Reprinted with permission from [68]. Copyright 2009 American Chemical Society.

include poor resolution, high operating voltages, and slow circuit speeds. Some of these disadvantages have been overcome using the recently described self-assembled printing technique which benefit from efficient formation of a self-assembled monolayer of 1H,1H,2H,2H-perfluorodecanethiol during the process [65,66].

Perylene alkyldiimide derivatives (PDIR) are among the most promising candidates to develop high-performance *n*-type OFETs as they exhibit one of the highest charge-carrier mobility among organic semiconductors [67]. Due to the intrinsic OFET operating principles, a small variation in semiconductor aggregation can induce a large variation of electrical properties. This is clearly demonstrated by the fluorocarbon functionalization of the PDI aromatic core (Compounds **1** and **2**, Fig. 2) which leads to a 10-fold enhancement of the electron mobility, attributed to the observed face-to-face molecular self-organization which accounts for the efficient excimer formation in comparison with the analogous hydrocarbon derivative.

Hydrogen-bonding (H-B) can be used as a secondary interaction to construct supramolecular architectures since they are highly selective and directional. In that regard several examples where π–π interactions and hydrogen-bonding are combined have been reported. Control of thin film morphology by self-assembly using H-B, has been obtained for *n*-type semiconductors such as perylenebisimides (PBIs) and also *p*-type oligo(*p*-phenylenevinylene)s (OPVs) in solution prior to processing [69]. The resulting films mainly consist of uniform rod-like domains. These architectures lead to enhanced charge-carrier mobility in comparison with films processed from dissolved molecules. Connecting the PBI and OPV units through a complementary network of H-B allows the formation of dyads which stack co-facially. These supramolecular structures exhibiting two independent pathways for charge transport, allowing for the construction of an ambipolar field-effect transistor. In contrast, suppressing the H-B motifs leads to charge-transfer donor–acceptor complexes between the PBI and OPV units which do not show any mobility in FET devices.

Self-assembly of 1-pyrenyl phosphonic acid (PYPA) through strong H-B and π–π stacking has been exploited by Yip et al. to create controlled 2D architectures consisting of laminate bilayers [70]. The supramolecular organisation occurs during the spin-coating process at the air/alcohol interface during which the pyrene moieties form π–π stacks with each other. The resulting hydrophobic layer points toward the sol–air interface whereas the phosphonic acid groups form a network pointing towards the solution. By repeating this process, laminated structures are formed and can be transferred onto SiO_2/Si substrates for the construction of OFETs in which PYPA assemblies act as an efficient *p*-type semiconductor.

Surface chemistry can also dictate the properties of nanoscale devices. Nanotube-based FETs have been found to be very sensitive to the interaction of single-walled carbon nanotubes (SWNTs) and the molecular species in their environment. The water molecules present on the SiO_2/Si substrate in a TC/BG configuration induce hysteresis of electrical characteristics due to charge trapping [71]. This phenomenom can be suppressed by surrounding the SWNT by poly(methylmethacrylate) (PMMA) which forms H-B with the silanol groups of the surface. Amphiphilic heteroleptic tris(phthalocyaninato) europium complexes have been utilized as

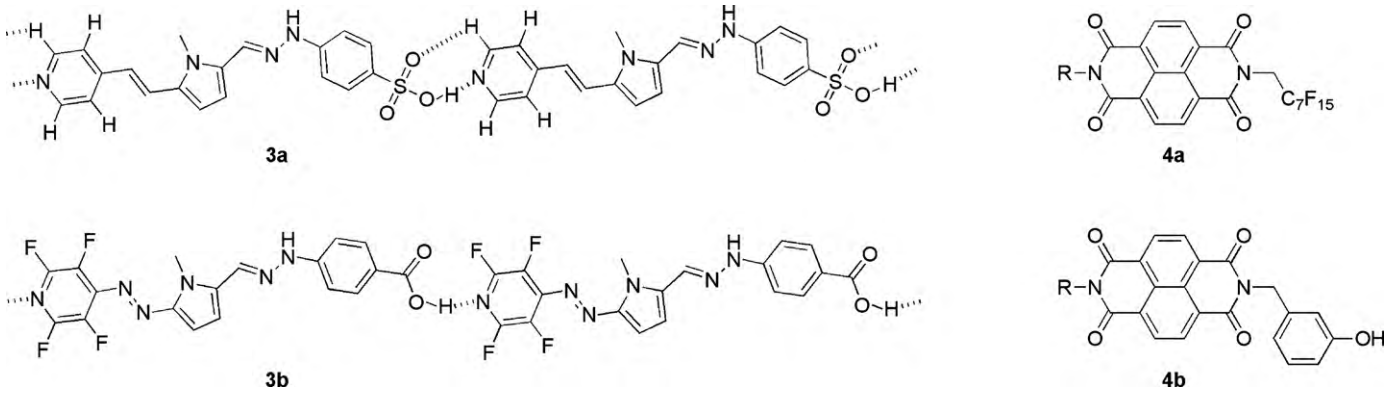

Fig. 3. Examples of H-B materials used for the fabrication of nanodielectric thin films by vapor-phase deposition (**3**) [74] and for imparting molecular recognition capabilities to the active layer of an OFET device (towards dimethyl methylphosphonate in the case of **4b** [77]).

triple-decker-shaped semiconductor [68]. A TC/BG OFET configuration was fabricated using a SiO_2/Si substrate, and the performance was found to be strongly controlled by the size of the crown-ether ring. For example, the formation of edge-to-edge *J*-aggregates was observed for the 12-crown-4 derivative, whereas face-to-face *H*-aggregates are obtained for the structure bearing a 18-crown-6 (Fig. 2).

Inorganic (SiO_2) or polymer insulators are commonly used as gate dielectrics. For OFET applications, it is known that in addition to the dielectric surface roughness, current leakage through the gate insulator has significant consequences on performance. Recently, molecule-based dielectric films with large permittivities (k) have attracted attention as they enable lower operating voltages and reduced power consumption [59,72]. Their optical-transparency, processability and flexibility, as well as improved compatibility with organic semiconductors are the principal advantages of organic gate dielectrics [40]. The controlled self-organization of ordered materials for gate dielectrics has been achieved from the self-assembly of precursors *via* H-B interactions. Thus, highly polarizable π-conjugated stilbazolium units have been designed to self-assemble *via* head-to-tail intramolecular H-B between pyridine or fluorinated pyridine and sulfonic or carboxylic acid end groups, respectively, leading to self-ordered thin films (**3**, Fig. 3) [73,74]. These self-assembled nanodielectrics (SAND) were subsequently capped with SiO_2 and the resulting organic–inorganic hybrid films display smooth surface morphologies, as demonstrated by AFM measurements. Moreover, the selected donor–acceptor π-conjugated functionalities also participate to the electronic polarizability enhancement and lead to a high k bulk layer. Pentacene OFETs based on v-SANDs fabricated by vapor deposition process thus exhibit excellent performance at low operating voltages. It is noteworthy that deoxyribonucleic acid (DNA) was also recently used as a gate dielectric, thus demonstrating the suitability of OFETs as biosensors [75,76].

Organic field-effect transistors offer great promise for applications in chemical sensing in which there is a need for small, portable and inexpensive sensors. OFET-based sensors utilize a functionalized thin film of organic semiconducting material as the active layer of a field-effect transistor that is exposed to the analyte on one side and to a gate electrode separated by an insulator on the other side. The electrical response is easily measured with simple instrumentation. As already mentioned, the mechanism of charge transport is complex and depends drastically on the structural organization of the material because intrachain conjugation defects require hopping of the charges between adjacent chains. One key advantage of OFET sensors is that a gate-induced accumulation layer at the insulator/semiconductor interface of OFETs greatly increases the conductivity (s) of the sensor material. In these devices, the OFET source–drain current (I_{SD}) is monitored at fixed source–drain (V_{SD}) and gate (V_G) voltages, as a function of the exposure to analyte molecules. As introduced by Torsi et al. [78] fully characterized OFETs offer access to more sensing parameters than just I_{SD}. Analysis of the saturated transfer characteristics of the OFET allows for the separate extraction of the carrier mobility, μ, and threshold voltage, V_T; other parameters, such as the conductivity at zero or reverse gate bias (depletion), are also readily accessible.

The capacity to fabricate self-assembled three-dimensional (3D) structures will be potentially useful for the development of sensory elements [79]. It is expected that selected objects, for instance micro- or nanospheres, functionalized with molecules that can direct their self-assembly through H-B, electrostatic or hydrophobic–hydrophilic interactions, are needed to prepare controlled 3D assemblies. The self-assembly sites can be introduced *via* chemical modification on exposed areas of spheres after a sequential process of spin coating and etching of a photoresist; or alternatively a metal layer can be first deposited and subsequently the desired functional moieties can be introduced. Along such lines, Bao et al. prepared SiO_2 spheres with patterned gold caps which were grafted with complementary strands of DNA used as self-assembled linkers [80].

The application of OFET as chemical sensors has been investigated considerably in recent years. Molecular engineering based on supramolecular interactions is of special interest to achieve specific and enhanced sensing properties. Katz et al. recently reported an OFET device in which the semiconducting layer was composed of a naphthalene-1,4,5,8-tetracarboxylic diimide layer subsequently covered by a modified semiconductor bearing a phenolic recognition unit chosen to specifically target dimethyl methylphosphonate (compounds **4a** and **4b**, Fig. 3) [77]. The receptor semiconductor was deposited as an island overlayer in a bilayer film device based on a perfluorooctylnaphthalene tetracarboxylic diimide (NTCDI). The effectiveness of the polar phenol groups in forming a hydrogen bond with DMMP forces guest molecules to become entrenched on the surface, where they proceed to drastically inhibit current flow between the source and the drain electrodes.

The microelectronics industry is still pushing towards inexpensive and lightweight devices constructed from low-cost materials. In that direction, the possibility of using multilayer mechanically compacted natural cellulose fibers as structural support and gate dielectric for *n*-type OFETs paves the way to low-cost high-performance devices [81]. The TC/BG configuration paper-based FET were prepared from long pinewood fibers that strongly associate through a H-B network, which were mixed with polyester fibers before subsequent deposition of patterned metal layers as source and drain electrodes.

3. Supramolecular materials for organic light-emitting devices

3.1. OLEDs

The easy processability of molecular materials along with tunable colours across the visible spectrum make molecule-based systems potential candidates for materials for organic light-emitting diode (OLED) devices for large, flexible, lightweight, flat-panel displays as well as for lighting applications [82]. Examples are already known in cell phones and digital cameras [83]. Such devices in their most rudimentary form consist of one or several semiconducting organic layer(s) sandwiched between two electrodes. However, the exacting requirements in terms of hole and electron injection, transport and luminescence efficiency/quantum yield has led to the development of multilayer, multimaterial structures, as an ideal multimodal material is unknown [84]. Most highly fluorescent or phosphorescent materials for OLEDs tend to have either *p*-type (hole transport) or *n*-type (electron transport) charge transport materials leading to poor efficiency and brightness in single layer devices, which can be overcome by adding an electron-transporting material adjacent to the cathode and/or a hole transporting material adjacent to the anode [85,86]. When an electric field is applied to an OLED, electrons are injected from the cathode into the lowest unoccupied molecular orbital (LUMO) of the adjacent molecules, concomitant with holes being injected from the anode to the highest occupied molecular orbital (HOMO). The two types of carriers migrate towards each other, some of which recombine to form excitons, a fraction of which decay radiatively to the ground-state emitting light. As such, charge recombination leading to light emission is the corollary of photovoltaic materials, treated in section 4, thus many concepts introduced in this section are equally applicable in photovoltaic devices. Related electrochromic displays possess an advantage over other technologies because it is possible for a single electrochromic pixel to produce multiple colours in addition to white, depending on applied potential.

Supramolecular interactions can potentially come into play in active layers by enhancing electron and hole transport, as well as assuring stability and even colours obtained (pure colours to white light). Structuring active layers as detailed below can be achieved either by layer-by-layer deposition or optimizing intimate mixing of materials. Stokes shifting of emission may be expected in certain cases, and significant progress has been made recently in developing phosphorescent emitters *via* triplet–triplet energy transfer [87]. Several growth methods for the active layers are described in the sections below, additionally we can cite a range of growth strategies (e.g. oblique incidence molecular beam deposition, hot-wall deposition) for the growth of molecularly ordered thin films [88]. Equally, the strong tendency of organic and organometallic nanoparticles/molecular clusters to rapidly self-assemble into highly aligned, stable superlattices at room temperature when solution-cast from dispersions or spray-coated directly onto various substrates was harnessed in OLEDs [89]. For example *via* a precipitation process based on rapid expansion of a supercritical CO_2 solution, it was believed to result in molecular distances and alignments in the nanoparticles that are not normally possible – hence the extreme longevity of these van der Waal's complexes. Functional OLEDs, which have the same host-dopant emissive-material composition with process-tunable electroluminescence (e.g. green to yellow), have been built with these nanoparticles, indicating the presence of novel nanostructures. Other techniques used in depositing conjugated polymer films for use in light-emitting devices include hybrid inkjet printing [90–92], bar-coating [93], electrophoretic deposition of nanoparticles [94], microcontact printing [95], screenprinting [96–98], electrophoretic deposition from suspension [99], and the use of liquid buffer layers to permit sequential deposition of multiple polymer layers without disturbance of previously deposited layers [100] have been described, and the inkjet printing method is now being extensively developed in industry [101,102]. These can be combined with the more traditional methods for making devices.

Once dissolved in nematic liquid crystals, poly(arylene vinylene)s and poly(arylene ethynylene)s form highly ordered structures which might offer a new way to obtain highly ordered films of polymers [103]. One promising area for future research concerns construction of nanosized LEDs, as it has been shown that decreasing LED size can improve device efficiency and lifetime [104]. Nanopatterning ITO by electron beam lithography enables LEDs to be made with emission coming from regions of approximately 170 nm in diameter [105]. Whether advances in nanotechnology will enable even smaller devices to be made and integrated with other nanosized electronic devices promises to be one of the most interesting and potentially exciting areas in LED research in the near future. For a comprehensive review on conjugated polymers for OLEDs see reference [106].

In layer-by layer (LBL) assembly, a thin film is grown up on a substrate surface by alternating its exposure to aqueous solutions containing differently charged (positive or negative) species [107–110]. The most commonly employed LBL assembly interactions are electrostatic, where a film is created by combining a polycation and a polyanion [111]. Films created by LBL assembly are inherently two-component composites and can be designed to provide additional functional performance. This technique has been employed to create high-quality electrochromic electrode films [112]. Full exploitation of the technique by the combination of two similarly colouring electrochromic materials has resulted in electrode films possessing extremely high contrast [113].

A recently reported proof-of-principle multiply coloured electrochromic electrode was based on LBL assembly [114]. The electrode films were created by exploiting electrostatic attractions between the polycation poly(aniline) (PANI) and a negatively ionized Prussian Blue (PB), iron(III) hexacyanoferrate(II) nanoparticle dispersion. The organic/inorganic nanocomposites show a linear increase in film thickness with successive, alternating assembly exposure steps. Electrochemical and spectrophotometric characterization confirms the distinct and non-interacting contributions from PANI and PB and reveals that both are fully electrochemically accessible even in relatively thick films. While PANI changes from a colourless reduced state (leucoemeraldine salt) to a green/blue oxidized state (emeraldine salt), the PB nanocrystals change from a colourless reduced state (Prussian White, PW), to a deep cyan oxidized state. These transitions occur over the same potential range: −0.2 to 0.6 V *vs.* K-SCE. PANI passes through a yellow intermediate state while the PB passes through a pale blue intermediate state. As a result, due to colour mixing, the PANI/PB composite should be nearly colourless at −0.2 V, pass through a green intermediate state, and finally become blue at 0.6 V. This strategy possesses an advantage over electrochemical deposition because the PANI chemistry and PB crystal size can be precisely controlled. The formation of nanometre scale PB crystals in solution, thereafter combined in a LBL assembled film with a polyelectrolyte, results in a faster switching and higher contrast electrode film than can be prepared by electrochemical means [115].

A different system using electrostatic interactions is based on polyoxometalate–polyelectrolyte hybrids, giving rise to a novel design for a dual-mode photo- and electroactive device that combines the ease of fabrication and flexibility of polymeric materials with the high photo- and electrochemical stability of inorganic materials [116–118]. The coating reversibly changes colour from transparent to blue by photo- and/or electroinduced stimulation when Preyssler-type POM, $(NH_4)_{14}[NaP_5W_{30}O_{110}]$ and

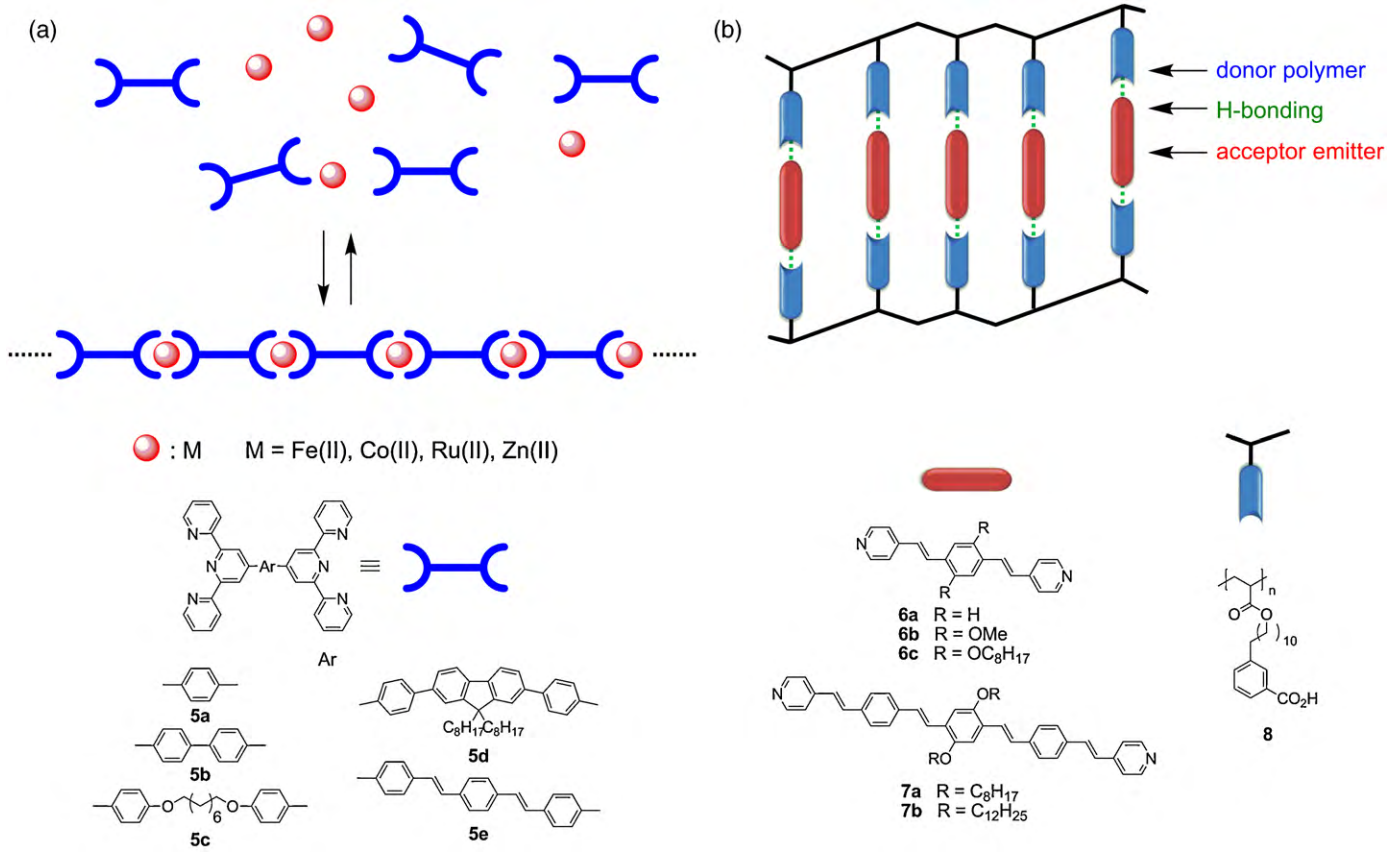

Fig. 4. (a) Metal directed formation of electroluminescent architectures; (b) ideal hydrogen-bonding ladder-like structure combining H-bonding polymer backbone with H-bonding rungs [124]. (b) Ladder-like structures formed *via* H-B interactions [127].

polyelectrolyte poly(4-vinylpyridine) (P4VP) are employed. The polyelectrolyte serves a dual role as a proton reservoir needed for the photochromic response and as a positively charged matrix to immobilize the anionic cluster [119–121].

An all-organic version of polyelectrolyte assemblies is also available based on self-assembled poly(4-vinyl pyridine) (P4VPy) with poly(N-vinyl carbazole) (PVK) and 2-(4-biphenylyl)-5-(4-tert-butyphenyl)-1,3,4-oxidiazole (PBD) as transport layers. The self-assembly is based on the electrostatic attraction of oppositely charged polymers formed by successive dipping in 0.01 M solutions. This self-assembled methodology allows fabrication of alternating multilayers, not only by the poly(phenyl vinylene) (PPV) and derivatives, but also by partial protonation of P4VPy, by which the charge on P4VPy is generated by the protonation process. The multilayered structures are characterized by specular X-ray reflectivity, UV absorption, photoluminescence and electroluminescence. The most efficient OLED device configuration found was: ITO/PVK/assembly/Al; (assembly = $[P4V(Py/Py1)/SPS]_n$); SPS = poly(sodium *p*-sulfonate styrene). Electrostatic attraction assembly allows fabrication of highly regular, alternating multilayers by the partial protonation of P4VPy, widening the scope of polymers suitable for applicable for use in OLEDs. As well as main-chain π-conjugated polymers, such as the PPV precursor and derivatives, luminophore containing side-chain polymers, as in the case of partially protonated P4VPy, can be used as the active component in OLEDs [122].

A wide range of supramolecular edifices of different topologies have been obtained under thermodynamic and kinetic control by metal-to-ligand coordination, including helicates, molecular machines and linear coordination polymers [123]. Concerning this latter type, organic–metallic hybrid polymers are formed by the complexation of metal ions with organic ligands or polymers bearing coordination sites.

The first such materials reported were the luminescent polymers based on **5c**–**5e** (Fig. 4**a**) formed by self-assembly of the emissive units through metal complexation between the terpyridine ligands at each end of the chromophore and zinc ions [124]. Their photoluminescence (PL) maxima range from 450 nm for **5c** to 567 nm for **5e**. Polymers **5c** and **5d** have been used to make blue (λ_{max} = 450 nm) and green (λ_{max} = 572 nm) emitting LEDs, respectively, which display only moderate electroluminescence (EL) efficiencies. Hybrid polymers consisting of bis(terpyridine)s **5a** and **5b** and metal ions such as Fe(II) or Ru(II) have specific colours based on metal-to-ligand charge-transfer (MLCT) absorption and emission. The cyclic voltammograms of the polymers revealed a reversible redox wave that depends on the redox reaction of the metal ions. Solid-state devices based on polymer films cast on indium-tin-oxide (ITO) electrodes display electrochromic properties; the colour of the film disappears when a potential higher than the redox potential of the metal ions is applied to the polymer film. Various colours such as purple, blue, red, and orange can be observed by changing the metal species and/or by modifying the organic ligands used to synthesize the polymers. In addition, multicolour electrochromic changes in a polymer film occur upon the introduction of two types of metal ions into the polymer [125]. Supramolecular organic light-emitting diodes were obtained using an aluminium chelate with a calix[4]arene complex thin film as emitter and electron-transporting layer. The devices were grown onto glass substrates coated with an indium-tin-oxide layer and aluminium cathode. On applying a dc voltage between the device electrodes in forward bias condition, a blue light emission in the active area of the device was observed. It was found that the electro-

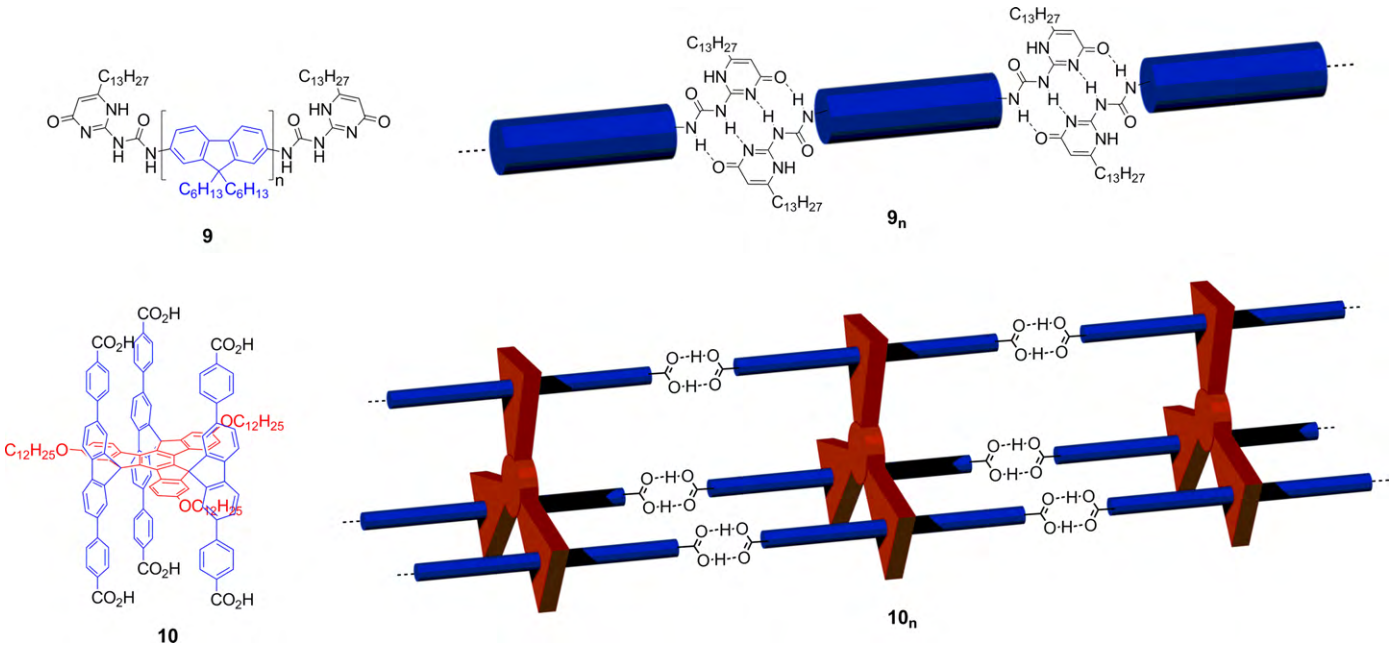

Fig. 5. 1D emissive polymeric systems/nanowires based on terminal H-bonds associating small oligomers [131,135,136].

luminescent emission peak can be tuned between 470 and 510 nm changing the applied voltage bias from 4.3 to 5.4 V [126].

The energies of H-bonds (25–40 kJ/mol) are significantly weaker than ionic bonds (200–400 kJ/mol) but stronger than van der Waals interactions (5–10 kJ/mol) [128,129]. Mesomorphic and photophysical properties of H-bonded polymer networks and trimers can be easily adjusted by tuning the H-bonded donors (donor polymers, **8**) and acceptor emitters in the H-bonded complexes (**6**, **7**). As illustrated in Fig. 4b, combining hydrogen-bonding polymers with complementary smaller bridging molecules is anticipated to lead to comb-like structures, which unlike small molecule analogues have proven to form uniform films [127]. Mesomorphic properties may be introduced into these supramolecular structures containing non-mesogenic acceptor emitters. In addition, the emission properties of bis(pyridyl) acceptor emitters can be manipulated by their surrounding non-photoluminescent proton donors. Compared with pure bis(pyridyl) acceptor emitters, red-shifts of emission wavelengths occurred in all blend films in poly(9-vinylcarbozole) PVK (dopant emitter: PVK 5:100 wt%) showing blue to green light emission. Luminescence spectra of fully H-bonded complexes of bis(pyridyl) acceptor emitters with m-PC10BA (molar ratio = 1:2) are even widely distributed from blue to red colours (from 396 to 642 nm). A very narrow fwhm value (38 nm) of EL emission can be obtained in the H-bonded complexes blended with PVK, and higher brightness of EL is produced at an appropriate annealing temperature. These systems were further elaborated on incorporating electron-transporting dendritic H-donors in addition to the light-emitting H-acceptors [130].

On the other hand, structurally rigid emissive molecules (**10**), comprising a planar polyaromatic stage and three α,ω-terminated biscarboxlate stilts were shown to self-assemble using H-bonds from the latter on each terminus to form a 1D-vermicular structure with pure blue luminescence due to the presence of 9,9′-spirobifluorene-like units [131]. Spiro compounds as organic molecular materials have become promising candidates for optoelectronic devices [132–134]. This supramolecular polymer was constructed by multiple hydrogen bonds and can form uniform nanowires with high aspect ratio and high solid-sate quantum efficiency (22%). Previously the authors showed the readily modifiable shape-persistent three-dimensional (3D) skeleton was facilely developed for organic light-emitting diodes and the construction of nanocages [131,135]. Another example of a hydrogen-bonded 1D-assembly is based on oligofluorenes **9** (n = 1–7), see Fig. 5. These species display blue PL (λ_{max} = *ca.* 410–420 nm) in the solid state, whose EL properties have yet to be reported [136].

Other optoelectronic devices employing H-bonding include the NLO properties of hydrogen-bonded thin films, such as those based on 5-bromo-5′-formyl-2,2′-bithiophene-4-nitrophenyl hydrazone (BITINPH) molecules [137]. Indeed, in addition to a large molecular hyperpolarizability, the second-order macroscopic nonlinearities are strongly dependent on the relative arrangement and orientation of the π-conjugated chromophores in the bulk solid state, and prevent unwanted anti-parallel dipole–dipole aggregation.

3.2. Light-emitting electrochemical cells

A more recent type of luminescent device which has attracted a lot of interest are polymer-based light-emitting electrochemical cells (LECs). Some examples of emissive polymers are shown in Fig. 6. In these devices, the luminescent material is mixed with an electrolyte [138]. Overall performance is linked to, for example, non-covalent electrolyte-polymer interactions. LECs show some marked differences in their behaviour from LEDs, see reference [139] for a detailed discussion of the operating principles of LECs and their differences from LEDs. Some key points are non-rectifying current voltage characteristics and emission with similarly low threshold voltages under both forward and reverse bias, which are nearly independent of the film thicknesses. Efficiencies are also relatively insensitive to the work function of the electrodes. Prototypes consisted of a conjugated polymer blended with poly(ethylene oxide) (PEO), a well-known charge-transporting polymer, and lithium triflate (LiOTf), sandwiched between ITO and aluminium electrodes [140–143]. Red-orange, green, and blue emission were obtained using different polymers [144]. The devices operated by production of *p*- and *n*-doped layers at the anode and cathode, respectively, which extend toward the center of the layer to form an internal *p*–*n* junction where recombination and emission occur.

The efficiencies of LECs are sometimes much higher than the optimal values for LEDs using the same emissive polymer and

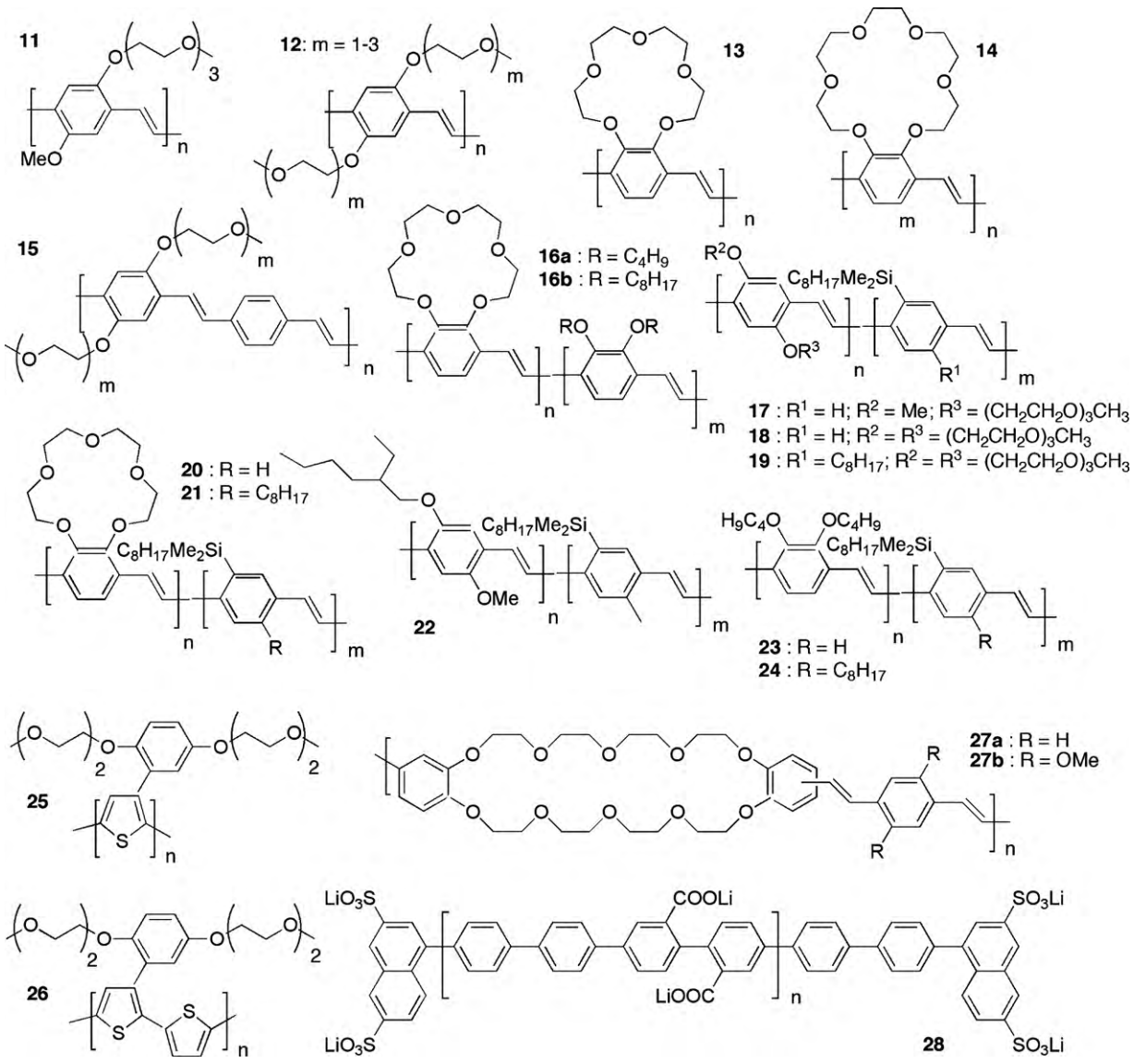

Fig. 6. Some ion/electrolyte sensitive emissive polymers used in light-emitting devices.

onset voltages for LECs can also be much lower than those for the corresponding LEDs. PEO can be omitted when the polymer is appropriately substituted, e.g. with ethylene oxide or crown-ether substituents. A variety of PPV derivatives with PEO or crown-ether substituents have been made and used in LEDs and LECs. Generally, they show much lower onset voltages and higher EL efficiencies in LECs than in LEDs. The homopolymers **11**, **12** and **14** show red-orange emission [145–147], while the alternating copolymers **15** show yellow-green emission (λ_{max} = 552 nm) [148,149]. The luminescence efficiency of polymer **13** has been improved by copolymerization with alkylsilyl- or 2,3-dialkyloxyphenylenes [150–152]. Thus, the copolymers **16** show solid-state PL efficiencies of 38% (**16a**) and 52% (**16b**), respectively (cf. 9% for homopolymer **13**). As might be expected given their good ion transporting properties, these copolymers give better performance in LECs than in LEDs.

A LEC using a blend of homopolymer **12b** and copolymer **15b** displays bias dependent emission, with the copolymer emitting under forward bias and the homopolymer under reverse bias [153]. The SiPPV copolymers **17**–**19** show similar emission spectra with much higher EL and PL quantum efficiencies than those of the homopolymers **11**, **12** [145,154–157]. The crown-ether substituted PPV copolymer **20** gave a green emitting (λ_{max} = 515 nm) LEC [150,152]. The addition of PEO was found to markedly increase the EL efficiency and response time of the device, as the crown-ether units lowered the ion mobility. The crown-ether-PPV copolymers **20**, **21** show green luminescence (λ_{max} = 555 and 549 nm, respectively), again with much better PL efficiencies (48% and 28%) than those for the homopolymer **13** (9%). Different EL efficiencies were obtained with aluminium (1.4%) and calcium (0.7%) cathodes for **22** [150,152]. The copolymers **17**–**19**, **23**, **24** show better performance in LECs.

Red-orange emitting LECs have also been made using polythiophenes **25**, **26** with ethylene oxide substituents [158]. Polymers containing arylene vinylene chromophores linked by ethylene oxide, or crown-ether spacers in the polymer backbone, e.g. **27**, have also been used to make blue or blue-green emitting LECs [159–162]. Efficiencies of up to 3.7 cd/A have been reported [163]. Conversely, it has been found that the lithium salts can be omitted from blends of PEO with polyrotaxanes formed by complexation of polymers, e.g. **28**, with cyclodextrin [164]. These blends produce much more efficient EL than the pure polyrotaxanes.

LECs often suffer from short shelf life and short operating lifetimes inhibiting commercial development in the near future. However, variants based on organometallic compounds may have

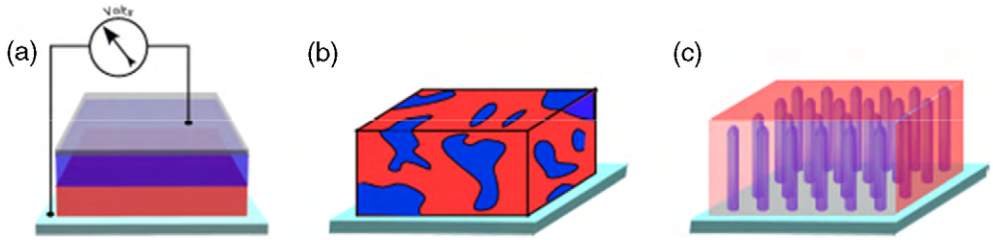

Fig. 7. Bilayer (a), bulk (b) and interdigitated (c) donor–acceptor heterojunctions.

a role to play in addressing many of the problems encountered with LEC devices [165–168].

4. Supramolecular materials for organic photovoltaic devices

It is widely accepted that the morphology of the active layer in organic photovoltaic (OPV) devices plays a crucial role in limiting the overall performance of the material [52,169–172]. In fact, the biggest single-step improvement in OPVs can be attributed to the introduction of the bulk heterojunction principle by Heeger in the 1990s (Fig. 7) [173]. Compared to bilayer devices, the leap in performance is attributed to greater contact between the electron donor and acceptor materials leading to more efficient charge separation. Combined with the latest-generation materials, this has allowed current technology to reach overall efficiencies of nearly 8% [174]. Still, the bulk heterojunction is far from the ideal interdigitated structure optimizing charge separation and collection (Fig. 7c). Moreover, its formation is controlled by the underlying chemical and physical properties of the materials, as well as by the technology and the conditions used for the deposition process and post-production treatment [175]. The biggest drawback is that each and every material must be optimized individually before its full potential can be assessed. In a seminal paper, Shaheen et al. showed that the performance of a material could be tripled by adopting conditions conducive to the formation of a fine-grain heterogeneous morphology [176]. Because the exciton diffusion length in organic materials is short, *ca.* 10 nm [177], the finer heterogeneous structure increases the probability that an exciton will encounter a discontinuity and dissociate into free charge carriers. In the case of devices based on poly-3-hexylthiophene (P3HT), thermal annealing is required to generate microcrystalline domains.

Supramolecular organization provides a direct method for assembling large numbers of molecules into structures that can bridge length scales from nanometers to macroscopic dimensions for efficient long distance charge transport [178,179]. This approach allows the design of extended complex structures built through the ordered assembly of elementary building blocks in solution prior – or during – the casting process using secondary interactions such as hydrogen bonding (H-B), electrostatic forces, π–π interaction, and CH/π interactions. However, only a few examples of solid-state all-organic photovoltaic devices incorporating designed supramolecular interactions have been reported to date.

Promising candidates include discotic liquid-crystalline materials based on extended π-aromatic structures (Fig. 8a), which can lead to the formation of 1D columnar superstructures that allow efficient charge transport [17,180]. The intermolecular attractive forces resulting from the large π-areas induce a pronounced

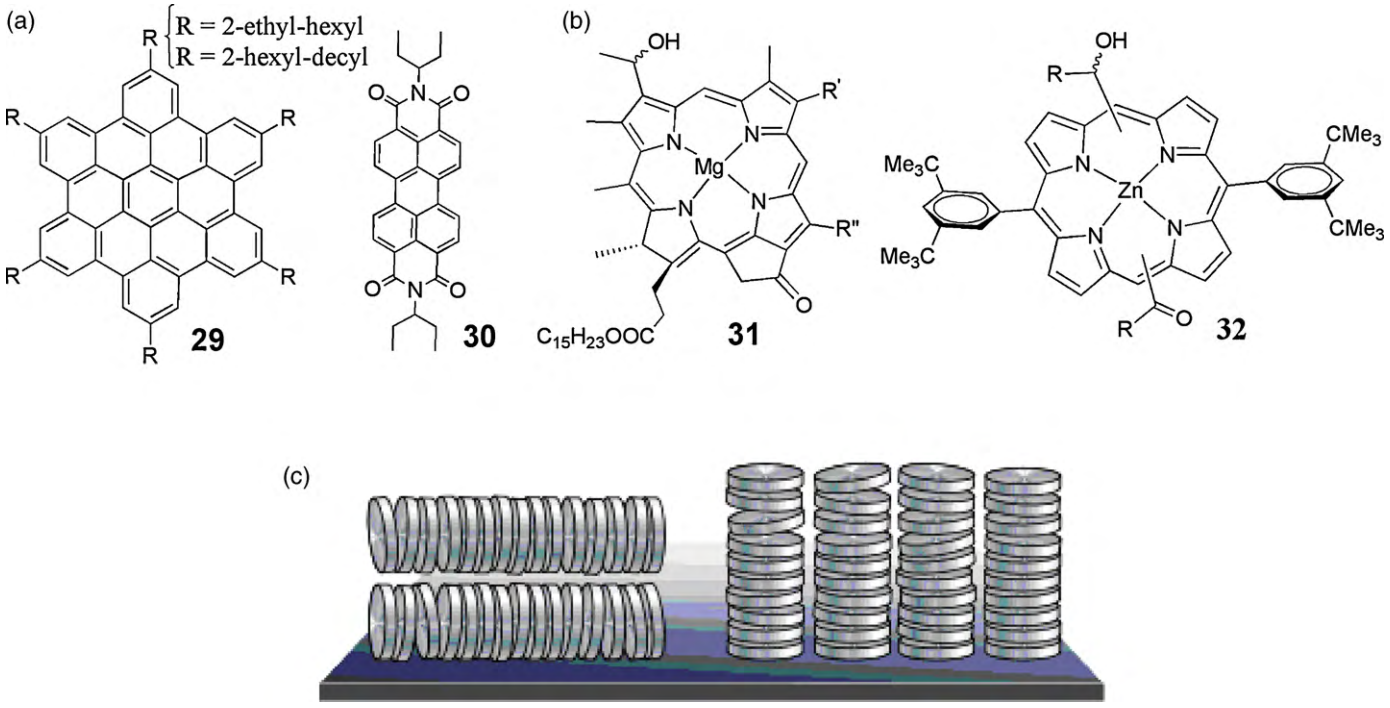

Fig. 8. (a) Example of an extended π-conjugated aromatic molecule capable of forming discotic liquid-crystalline phases suitable for the construction of OPV devices when blended with electron acceptor **30** [180]. (b) The natural self-assembling bacteriochlorophyll *c* (left) and a synthetic mimic (right) [181]. (c) Parallel (left) *vs.* homeotropic (right) arrangement of discotic liquid crystals.

propensity to self-assemble into highly organized structures. Balaban and co-workers have designed biomimetic chromophores (Fig. 8b) in which self-assembly can be controlled by adjusting the transition dipole moment [181,182]. The resulting supramolecular nanostructures are strongly fluorescent and not quenched upon anchoring onto nanocrystalline titania with different grain sizes, which makes them promising candidates for the fabrication of dye-sensitized solar cells. Specific helical assemblies of aggregated chromophores displaying strong electronic coupling (as evidenced by the formation of *J*-aggregates) were obtained using modified amylose polymers as templates [183]. Extended columnar architectures are equally interesting for the fabrication of OPV devices, provided that stacking of the material can be controlled to give columns that are formed orthogonal to the surface of the substrate (Fig. 8c). Homeotropic alignment can sometimes be favored by tuning the molecular structure [184], or surface modification [185]. Even when this is not the case, power conversion efficiencies of 1.5% were achieved despite a modest external quantum efficiency of 12% [180]. This suggests that considerable room for improvement is available by optimizing *inter alia* light absorption and device fabrication. Fullerenes possessing multiple aromatic substituents can align into columnar motifs in the solid due to hydrophobic interactions. Kennedy et al. showed that such architectures could be incorporated into solid-state photovoltaic devices, though the overall efficiency (*ca.* 1.5%) was still lower than analogous PCBM devices [186]. As often observed when supramolecular architectures are employed, thermal annealing had only a modest effect on the device properties.

Conjugated rigid-rod molecules provide convenient scaffolds that can be used to enforce the stacked arrangement of aromatic acceptor units while providing a pathway for hole transport. Synthetic accessibility and solubility limit the length of these covalent structures, but it is possible to use a combination of hydrophobic and electronic interactions to promote formation of interdigitated architectures spanning much greater lengths and incorporating chromophores covering a greater portion of the solar spectrum. By combining *n*-semiconducting NDI rainbow stacks and *p*-semiconducting rigid-rod scaffolds, the Matile group has developed programmed assembly of interdigitating intra- and interlayer recognition motifs on conducting surfaces [187–189]. These self-assembled zipper assemblies offer rapid access to supramolecular cascade *n*/*p*-heterojunctions exhibiting efficient photoconversion in photoelectrochemical set-ups.

Hydrogen-bonding interactions offer a convenient approach towards precisely controlling the geometry of electron donor–acceptor assemblies, and numerous conjugated polymers bearing H-B groups have been reported [50,190]. For example, triaminotriazine-substituted oligo (phenylene vinylenes) will bind perylene bisimides to form H-B trimers which then self-assemble into stacks conducive for charge separation (Fig. 9a) [178,191]. Besides perylene bisimides, other electron acceptors such as fullerene [192] and tetrathiofulvalene (TTF) [193] derivatives incorporating H-B units have been described, although self-doping behaviour, such as that observed for TTF-2-carboxylic acid in the presence of ammonia [194], may be a limitation.

Huang et al. proposed using non-self-complementary H-B interactions to direct the formation of supramolecular heterojunctions for photovoltaic applications [195]. Photoelectrochemical devices incorporating components possessing complementary H-B units were found to give a 2.5-fold enhancement in photocurrent compared to model systems in which self-assembly is suppressed. Subsequent improvement was sought by using hydrogen-bonding terminated self-assembled monolayers (SAMs) on gold, and the combination of a hydrogen-bonding barbituric acid appended fullerene and a complementary melamine-terminated thiophene oligomer to promote hierarchical self-assembly (Fig. 9b) [196]. The terminal thiol-group interacts with the gold surface resulting in the formation of self-assembled monolayers (SAMs) that are proposed to better accommodate the subsequent formation of the photo-/electroactive fullerene containing thin films due to complementary hydrogen-bonding interactions. Strong ground-state interactions between complementary H-B fullerene and oligoth-

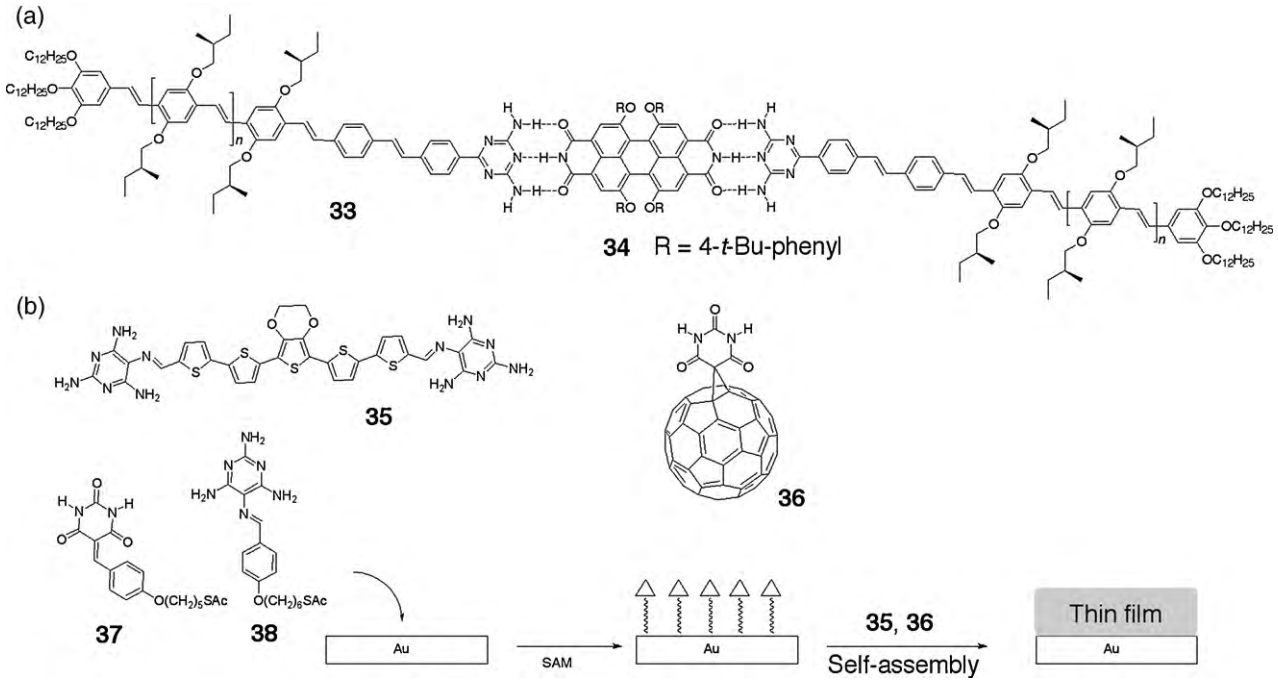

Fig. 9. Examples of H-B mediated self-assembly of donor–acceptor materials based on (a) OPVs and PDIs [178,191], and (b) oligothiophenes and fullerenes [195]. In (b), modification of the substrate with H-B motifs with preference for the donor or acceptor material was found to impact the performance of the device [196].

iophenes have been observed, and this may also contribute to the observed enhancement in photocurrent [197]. Intermolecular H-B interactions between a perylene tetracarboxylic dianhydride and a pentatiophene bearing terminal formyl groups was invoked by Jiang et al. to account for an increase in V_{OC} in flexible OPV devices [198].

Segregation at the molecular level can be controlled by covalently linking fragments possessing very different properties such as crystallinity and/or solubility. In the case of composite rod-coil polymer materials, the crystallization of the rigid-rod component is frustrated by the presence of a more voluminous and generally less well-ordered coil segment. This leads to molecular-level phase segregation, with the concomitant generation of relatively well-defined morphologies at the micron- and nanometer scale [199,200]. Application of this approach to controlling the morphology of polymer-based devices is usually based on the covalent attachment of flexible fullerene-rich polymers to the more rigid conjugated polymer segments [201,202]. However, difficulties in the synthesis and characterization of the materials make this approach very labor-intensive [203]. Recently, Hadziiannou and co-workers have turned to weaker non-covalent interactions between pyridine-containing polymers and C_{60} to supramolecularly introduce the fullerene component. The polymeric material consists of a poly(3-hexylthiophene) fragment connected to a poly(4-vinylpyridine) unit which, based on previous work by Ikkala and co-workers [204], is known to bind C_{60} through electron donor–acceptor interactions. Photovoltaic devices prepared by depositing such materials using spin-coating protocols and normal device architectures gave disappointing results, with overall efficiencies below 0.03%. Interestingly, detailed investigation of the active layer morphology by TEM indicated that a highly interpenetrated network of the donor and acceptor materials is indeed formed, but that the fullerene component preferentially accumulated in the vicinity of the PEDOT layer. The authors proposed that the basic sites of the poly(vinylpyridine)-containing material reacted with the acidic PEDOT-PSS layer, and proceeded to investigate the performance of inverted OPV devices (i.e. devices in which the anode is deposited on top of the active layer) in order to circumvent this problem. Indeed, the inverted architecture devices were found to display significantly enhanced performance (up to 1% conversion) compared to the above-mentioned normal architecture devices.

The introduction of single-walled carbon nanotubes (CNT) into polymer-based OPV devices has been investigated by numerous groups on the basis that the latter can significantly enhance charge transport within the active layer and may be less prone to phase separation than PCBM [205–209]. However, although difficulties in device fabrication arising from short circuits due to the presence of conducting CNT spanning the entire thickness of the semiconducting layer can be circumvented through the application of multiple layers, the presence of CNT invariably leads to a drop in overall efficiency ascribed to, amongst others, energy transfer quenching of the polymer-localized exciton due to the lower band gap of CNTs [210]. The concomitant use of PCBM and CNT was found to be beneficial to enhance the primary exciton dissociation step and devices incorporating CNT do indeed display a significantly enhanced current density, although this is insufficient to offset the reduction in V_{oc} [211]. In general, chemical or physical surface modification of the CNT is required to promote dispersion of the material during deposition (typically by spin-coating) and in the active layer of the device [210,212,213]. Stupp and co-workers have used non-covalent interactions between pyrene and CNT to assemble donor–acceptor architectures [214]. The pyrene-terminated pentathiophene donor was found to extensively coat the surface of the single-walled CNT to form concentric donor–acceptor double-cable architectures which were deposited onto transparent ITO electrodes by collecting the modified CNTs by filtration. The active layer was then covered with an additional layer of PCBM, but short circuits could not be entirely eliminated.

More precise control of the architecture of the active layer can be achieved by using molecular self-assembly to template the formation of small clusters of defined size and composition. These can then be cast from solution onto a transparent conducting electrode. Imahori et al. applied this technique for the formation of porphyrin – C_{60} clusters using H-B interactions [215] or Au nanoparticles (NP) [216] as templates. The resulting modified electrodes, when irradiated in a photoelectrochemical set-up using I_3^-/I_2 as an electron relay, exhibited maximum IPCE (incident photon to converted electron) efficiencies of 40–60%. Along similar lines, modified electrodes incorporating semiconducting CdS nanoparticles were prepared by self-assembly using complementary H-B interactions [217]. In this case, melamine- or barbiturate-capped CdS-NP was shown to bind to a gold electrode grafted with a thiol-SAM terminated with the complementary melamine or barbiturate unit. Additionally, a 2.6-fold enhancement in the observed photocurrent was noted when gold nanoparticles were incorporated between the macroscopic Au electrode and the CdS-NP.

To achieve directional energy transfer over long distances, Calzaferri et al. designed artificial photonic antenna systems based on the incorporation of chromophores inside metal oxide frameworks [218,219]. These architectures have received considerable attention for their potential in the fabrication of photovoltaic devices [220] because their supramolecular architecture leads to the electronic excitation energy being transferred to a well-defined location in the device through sequential resonant energy transfer. In this strategy, light-absorbing molecules are incorporated in the zeolite channels, which corresponds to a first stage of molecular organization. This allows light-harvesting within the volume of the host and radiationless energy transport along the channels. The second stage of organization involves the electronic coupling to an external acceptor or donor fluorophore (stopcock) at the channel entrances, which can then act as a sink to trap the electronic excitation energy. The third stage of organization is obtained by interfacing the material to an external device through the stopcock (Fig. 10).

Dye-sensitized electrochemical photovoltaic cell technology has been recognized as a viable alternative to the well-developed solid-state homo- and heterojunction solar cell technologies [221–224]. In this strategy, a network of titania nanoparticles serves as an electron-transporting medium and as a high-surface-area support for dye molecules capable of injecting electrons into the titana upon photoexcitation, and an electrolyte solution (typically aqueous I_3^-/I_2) is used to complete the electrical circuit. Continuous improvement in cell architecture and dye structure have brought the conversion efficiency up to 12% [224], but this could be further increased by augmenting the absorption envelope of the sensitizer and by diminishing unproductive charge recombination processes. Hardin et al. have recently reported that the use of ancillary light-harvesting dyes can lead to a 26% improvement in power conversion efficiency [225], and a similar enhancement was observed by Handa et al. when using donor–acceptor dye combinations [226]. Supramolecular chemistry, particularly of coordination compounds, has emerged as a viable route to preparing efficient dye sensitizers of greater complexity [227]. For example, ureido-pyrimidone H-B units can be incorporated in to a short polymer framework to prepare electrolytes that retain the rheological advantages of longer polymers while remaining small enough to fit inside the titania pores [228]. Covalent [229] and non-covalent [215,230] examples of multi-chromophore dyes exist, and the effects of H-B on the surface structure of TiO_2 were investigated by Imahori et al. [231].

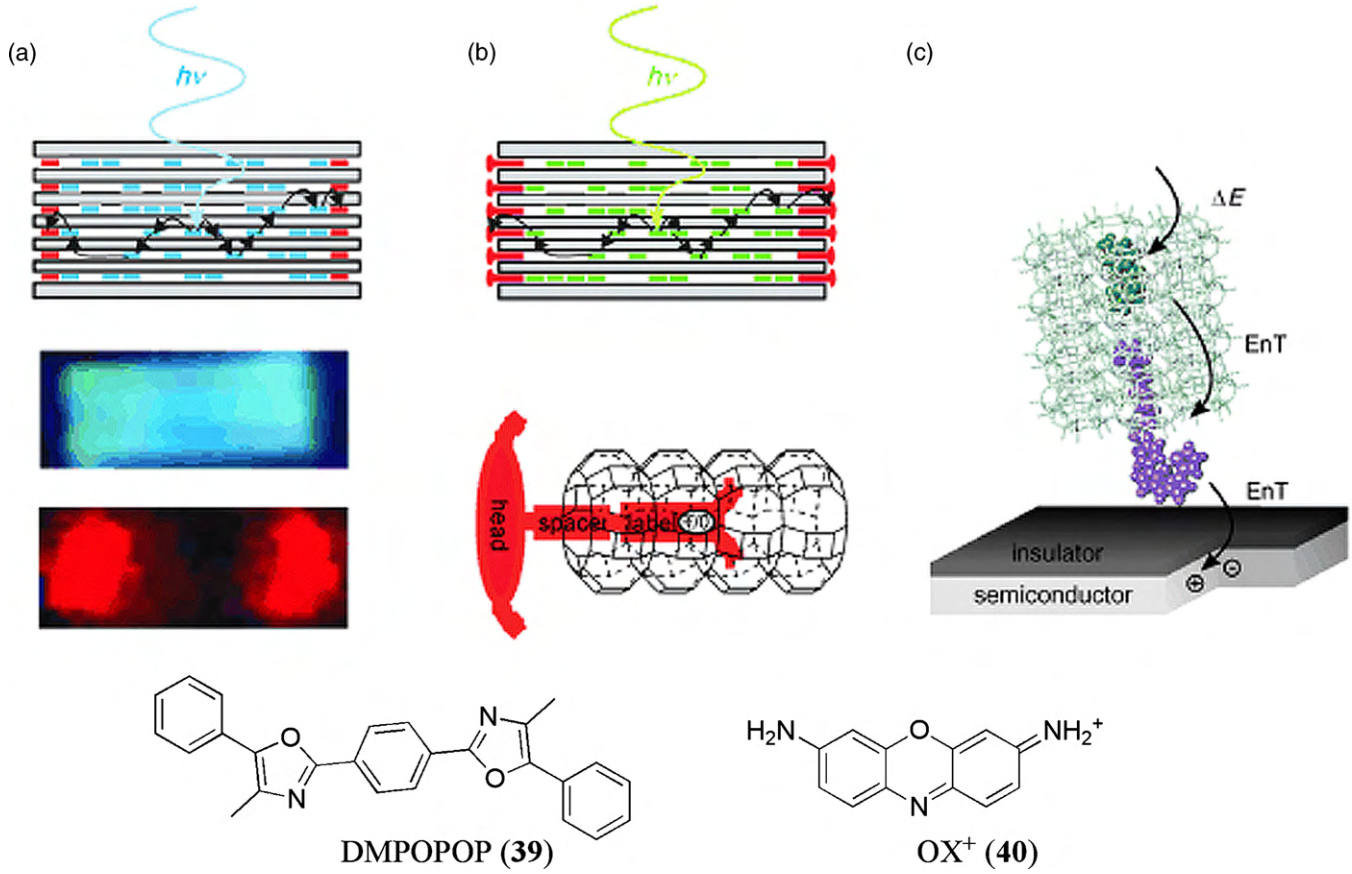

Fig. 10. (a) Dye-loaded zeolite L antenna; blue-emitting donors inside the zeolite transfer electronic excitation energy to the lower energy red-emitting acceptors located at the ends of the cylindrical crystal as shown by fluorescence microscope images of a 2 μm-long crystal containing DMPOPOP (**39**) in the middle part (blue, polarizer parallel) and Ox+ (**40**) at the ends (red, polarizer perpendicular) upon selective DMPOPOP excitation. (b) Antenna system with stopcock molecules as external traps and schematic representation of a stopcock at the end of a zeolite L channel. The stopcock consists of a head, a spacer, and a label. (c) Energy transfer (EnT) from a photonic antenna to a semiconductor, creating an electron–hole pair in the semiconductor (radiationless near-field process). Copyright Wiley–VCH Verlag GmbH & Co. KGaA. Reproduced with permission [218].

5. Supramolecular materials for storage and logic

Molecular materials, which can be switched between at least two stable forms, have been considered as potentially promising candidates for information storage, as well as logic components for over half a century. Their small size and inherent redox and optical properties offer a means to address and read and write with small quantities of molecules with low power consumption. Molecular switches and machines, particularly in solution, have been the subject of numerous reports, which have been reviewed extensively [232,233]. Fundamentals for solution-based logic systems have been established for a range of systems from primary logic gates, following on from the prototype molecular AND logic gate [234], to combinatorial circuit analogues including half- and full-adders and subtractors, multiplexers, demultiplexers, games as well as many others [235–238]. More recently, some effort has been devoted to moving beyond incoherent solution-based systems towards organized host media which may be exploited in specific future devices, to some extent in analogy to surface etched silicon surfaces in microelectronics. Incorporation of redox-active ruthenium and osmium molecules into monolayers at a surface (glass)–liquid interface, which are responsive to Fe^{3+}, Ce^{4+} and water inputs, is one example of a move in this direction [239]. A hybrid biological version of this system, also relying on a spectroscopic output is a microscale single layer memory based on virus-semiconductor quantum dot hybrids, the latter typically presenting high quantum yields [240]. Molecular machines, where movement of a discernable molecular subunit, within a mechanically interlocked molecular ensemble, can be controlled by an applied stimulus have equally moved from solution to surfaces [241,242]. For example, this surface localisation was put to work with a layer of photoswitchable rotaxanes whose hydrophobicity/hydrophilicity was governed by the position of a molecular ring on a molecular thread, governed by switching intramolecular hydrogen bonding and hence ring thread movements. As a result, the movement of a macroscopic load, a liquid droplet under light irradiation was guided through biased Brownian movement [243]. Rotary movement has also been described where deposition of a supramolecular six-position rotary device, porphyrin **41** on a Cu(1 1 1) surface leads to the formation of a regular self-assembled non-covalent nanoporous network with a single porphyrin on top of each pore. Not being directly on the surface, an unusual rotary behaviour is measured by STM. The authors envisage that sufficiently high activation energies to rotation may lead to technological applications [244]. Molecular logic elements and switches have also made the step towards lower dimensional materials. This includes 1D silicon nanowires decorated with fluorescent logic gates, responsive to ions such as mercury and protons and which is equally considered compatible with silicon-based semiconductor technology [245]. Zero dimensional metal nanoparticles have also been decorated with molecular switches as have micrometric latex beads [246,247]. In the latter system, the combination of multiple molecular logic elements allows unique labelling of a large population of miniscule objects of importance for identifying members of a combinatorial library.

While defined architectures and strategies have been identified and optimization is taking place for devices in many of the previous sections in this overview, the areas of storage and logic has produced many imaginative and elaborate systems, largely from a chemical perspective but which have been not been fully tested in solid-state devices. Indeed, many of the systems which have their basis in biological/biomimetic systems, or "wet" computation do not readily lend themselves to integration in solid matrices where diffusion of chemical inputs is hampered. All-optical photochromic systems and logic gates in the solid-state have been developed, but due to a lack of supramolecular interactions are considered beyond the scope of this article [248–250].

Therefore the range of fully solid-state supermolecule-based systems under consideration is relatively limited compared to the

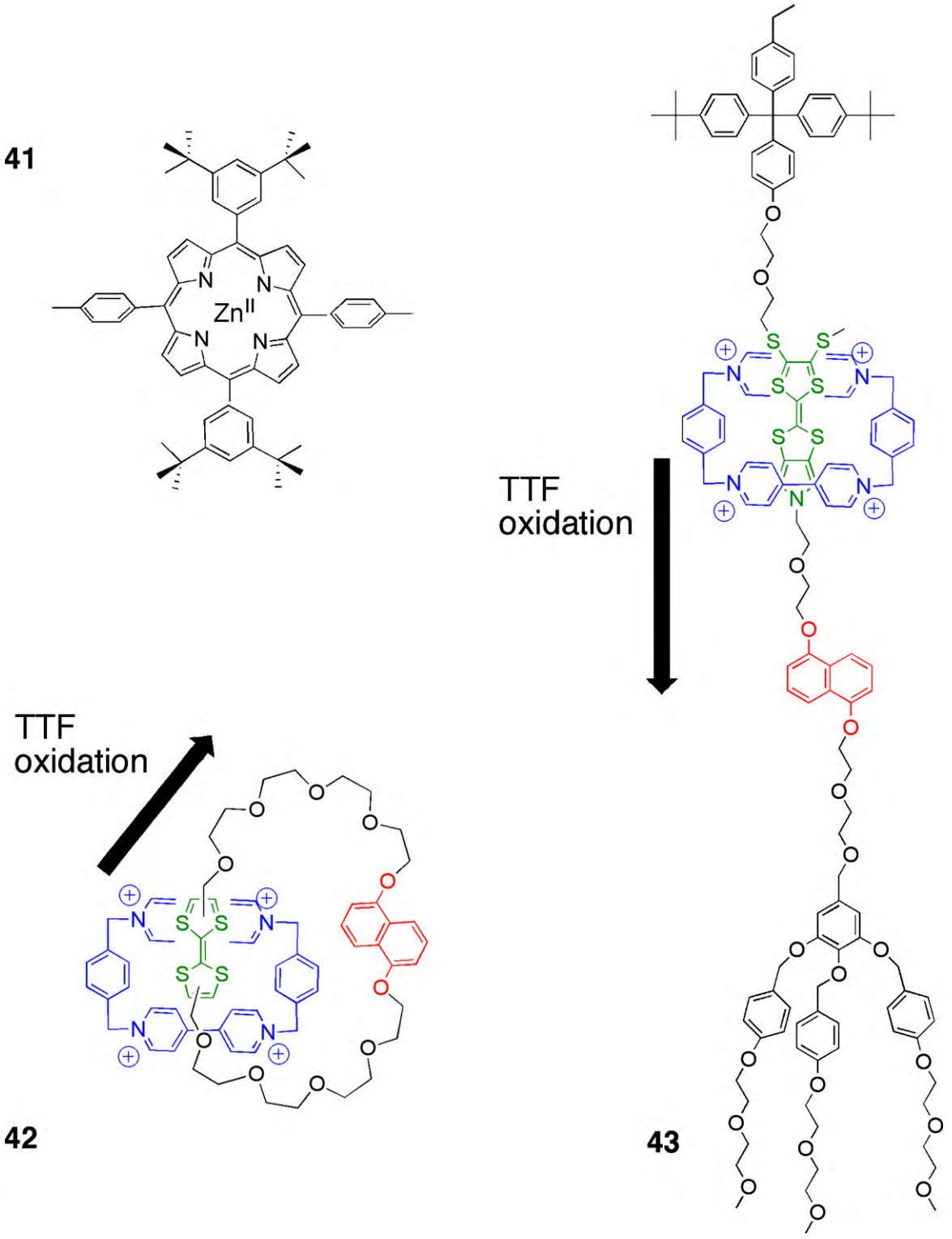

Fig. 11. Molecules showing rotational (**41** and **42**) and translational (**43**) switching [229,236]. Oxidation of TTF (green subunit) in **42** and **43**, when sandwiched between electrodes, results in reversible switching between two metastable forms of different conductivity [236,237].

solution-based cousins, and may be considered the least developed of current sections thereby representing an area for future work. Most effort in this domain has been dedicated to mechanically interlocked molecules where submolecular movement, in analogy to macroscopic counterparts, gives rise to the idea of molecular machines. Systems based on catenanes (comprising two or more interlocked molecular rings) and rotaxanes (where linear rather than rotary movement is noted through movement of a molecular ring on a molecular thread) have been considered.

A solid state, electronically addressable, bistable [2]catenane-based molecular switching device was fabricated from a single monolayer of the [2]catenane **42** (see Fig. 11), anchored with phospholipid counterions, and sandwiched between an *n*-type polycrystalline silicon bottom electrode and a metallic (Ti/Al:15 nm/100 nm) top electrode. The langmuir monolayers were prepared with 1:6 ratio of **42** $(PF_6)_4$: Na^+DMPA^- (1,2-dimyristoyl-sn-glycero-3-phosphate). Switching is achieved by oxidizing the electron-rich TTF unit destabilizing the interaction with the tetracationic ring provoking its movement to the dialkoxy naphthalene and leading to a detectable change in conductivity. The device exhibits hysteretic (bistable) current/voltage characteristics, with the switch being opened at +2 V, closed at −2 V, and read at around 0.1 V, and has been successfully recycled many times under ambient conditions [251].

Rotaxanes, considered more promising in the area of switchable molecular machine-based devices, have come into the fore in several recent examples of solid-state devices. An example is shown in Fig. 11 with **43** [252]. By integrating electrochemically switchable bistable [2]rotaxanes into nanowire crossbar arrays, large memory devices (160 kb) of unprecedented density, estimated at 10^{11} bits per cm^2 were fabricated and operated [252]. In this design, switching is achieved through similar electrochemically activated events described for catenane **42** above. Switching is achieved in the relatively small population (*ca.* 100 molecules) where the orthogonal bottom (Si 16 nm, 33 nm, *p*-doped) and top (Ti wire 16 nm, 33 nm pitch) nanowire electrodes cross. Characterization of the rotaxane in Langmuir–Blodgett monolayers and in the solid-state devices gave insight into the structure of the molecules in the device format. The relatively high number of identified defects could be isolated using software coding. The hysteretic changes in tunnelling current that form the basis of memory device operation resulted directly from the electromechanical switching process of the bistable [2]rotaxanes. Directionality is assured by preferential association of the poly(ethylene glycol) stopper units on the silicon surface.

6. Conclusion

A wealth of solution-based photo- and electroactive molecular compounds, polymers, machines and devices are known. However, relatively few of these systems have been integrated into solid-state devices. Inherent molecular properties and supramolecular interactions need to address stability and charge migration, which remain major challenges in the development of different device architectures including OFET, OLED and OPV. For real progress to be made in the field of supramolecular material-based electronic devices, closer work between chemists and laboratories/industries producing solid-state devices need to be fostered. The successful transposing of solution behaviour to the solid-sate bodes well for further solid-state devices based on these as well as other molecule-based systems.

Acknowledgements

Funding from the European Research Council under the European Community's Seventh Framework Programme (FP7/2007-2013)/ERC grant agreement no. [208702] is gratefully acknowledged. We also warmly thank the Région Aquitaine, the GIS Advanced Materials in Aquitaine, and the CNRS for financial support. L.J. and A.L.-C. thank the French ministry of education for Ph.D. grants.

References

[1] A. Aviram, M.A. Ratner, Chem. Phys. Lett. 29 (1974) 277.
[2] C. Joachim, M.A. Ratner, Proc. Natl. Acad. Sci. U. S. A. 102 (2005) 8801.
[3] C. Joachim, J.K. Gimzewski, Chem. Phys. Lett. 265 (1997) 353.
[4] S. Ami, M. Hliwa, C. Joachim, Nanotechnology 14 (2003) 283.
[5] I. Duchemin, C. Joachim, Chem. Phys. Lett. 406 (2005) 167.
[6] I. Duchemin, N. Renaud, C. Joachim, Chem. Phys. Lett. 452 (2008) 269.
[7] J.K. Gimzewski, C. Joachim, Science 283 (1999) 1683.
[8] C. Joachim, J.K. Gimzewski, A. Aviram, Nature 408 (2000) 541.
[9] R. Stadler, S. Ami, C. Joachim, M. Forshaw, Nanotechnology 15 (2004) S115.
[10] N. Weibel, S. Grunder, M. Mayor, Org. Biomol. Chem. 5 (2007) 2343.
[11] J.E. Green, J.W. Choi, A. Boukai, Y. Bunimovich, E. Johnston-Halperin, E. DeIonno, Y. Luo, B.A. Sheriff, K. Xu, Y.S. Shin, H.R. Tseng, J.F. Stoddart, J.R. Heath, Nature 445 (2007) 414.
[12] J.R. Heath, Ann. Rev. Mat. Res. 39 (2009) 1.
[13] F.C. Grozema, L.D.A. Siebbeles, Int. Rev. Phys. Chem. 27 (2008) 87.
[14] A.B. Mallik, J. Locklin, S.C.B. Mannsfeld, C. Reese, M.S. Roberts, M.L. Senatore, H. Zi, Z. Bao, in: Z. Bao, J. Locklin (Eds.), Organic Field-Effect Transistors, CRC Press, Boca Raton, FL, 2007.
[15] A.M. van de Craats, J.M. Warman, A. Fechtenköter, J.D. Brand, M.A. Harbison, K. Müllen, Adv. Mater. 11 (1999) 1469.
[16] I. Paraschiv, M. Giesbers, B. van Lagen, F.C. Grozema, R.D. Abellon, L.D.A. Siebbeles, A.T.M. Marcelis, H. Zuilhof, E.J.R. Sudholter, Chem. Mater. 18 (2006) 968.
[17] J. Wu, W. Pisula, K. Müllen, Chem. Rev. 107 (2007) 718.
[18] S. Kumar, Chem. Soc. Rev. 35 (2006) 83.
[19] S. Ghosh, X.Q. Li, V. Stepanenko, F. Wurthner, Chem. Eur. J. 14 (2008) 11343.
[20] Z.J. Chen, A. Lohr, C.R. Saha-Moller, F. Wurthner, Chem. Soc. Rev. 38 (2009) 564.
[21] S. Laschat, A. Baro, N. Steinke, F. Giesselmann, C. Hagele, G. Scalia, R. Judele, E. Kapatsina, S. Sauer, A. Schreivogel, M. Tosoni, Angew. Chem. Int. Ed. 46 (2007) 4832.
[22] W. Pisula, M. Zorn, J.Y. Chang, K. Müllen, R. Zentel, Macromol. Rapid Commun. 30 (2009) 1179.
[23] B. Schmaltz, T. Weil, K. Müllen, Adv. Mater. 21 (2009) 1067.
[24] S. Sergeyev, W. Pisula, Y.H. Geerts, Chem. Soc. Rev. 36 (2007) 1902.
[25] C.C. Chu, D.M. Bassani, Photochem. Photobiol. Sci. 7 (2008) 521.
[26] C.H. Huang, D.M. Bassani, Eur. J. Org. Chem. (2005) 4041.
[27] S. Burattini, H.M. Colquhoun, B.W. Greenland, W. Hayes, Faraday Discuss. 143 (2009) 251.
[28] D. Montarnal, F. Tournilhac, M. Hidalgo, J.L. Couturier, L. Leibler, J. Am. Chem. Soc. 131 (2009) 7966.
[29] P. Reutenauer, E. Buhler, P.J. Boul, S.J. Candau, J.M. Lehn, Chem. Eur. J. 15 (2009) 1893.
[30] I. Willner, B. Shlyahovsky, M. Zayats, B. Willner, Chem. Soc. Rev. 37 (2008) 1153.
[31] Z. Bao, J. Locklin (Eds.), Organic Field-Effect Transistors, CRC Press, Boca Raton, FL, 2007.
[32] C.D. Dimitrakopoulos, P.R.L. Malenfant, Adv. Mater. 14 (2002) 99.
[33] H. Sirringhaus, T. Kawase, R.H. Friend, T. Shimoda, M. Inbasekaran, W. Wu, E.P. Woo, Science 290 (2000) 2123.
[34] L. Torsi, A. Dodabalapur, Anal. Chem. 77 (2005) 380A.
[35] B. Crone, A. Dodabalapur, A. Gelperin, L. Torsi, H.E. Katz, A.J. Lovinger, Z. Bao, Appl. Phys. Lett. 78 (2001) 2229.
[36] H.E. Katz, Z.N. Bao, S.L. Gilat, Acc. Chem. Res. 34 (2001) 359.
[37] C.J. Brabec, N.S. Sariciftci, J.C. Hummelen, Adv. Funct. Mater. 11 (2001) 15.
[38] A.J. Heeger, Angew. Chem. Int. Ed. 40 (2001) 2591.
[39] M.M. Ling, Z.N. Bao, Chem. Mater. 16 (2004) 4824.
[40] C.D. Dimitrakopoulos, D.J. Mascaro, IBM J. Res. Dev. 45 (2001) 11.
[41] J. Zaumseil, H. Sirringhaus, Chem. Rev. 107 (2007) 1296.
[42] R. Ponce Ortiz, A. Facchetti, T.J. Marks, Chem. Rev. 110 (2010) 205.
[43] A. Facchetti, M.H. Yoon, T.J. Marks, Adv. Mater. 17 (2005) 1705.
[44] C.R. Newman, C.D. Frisbie, D.A. da Silva, J.L. Bredas, P.C. Ewbank, K.R. Mann, Chem. Mater. 16 (2004) 4436.
[45] F. Würthner, Angew. Chem. Int. Ed. 40 (2001) 1037.
[46] A. Kraft, Chemphyschem 2 (2001) 163.
[47] G. Wang, T.W. Kim, H. Lee, T. Lee, Phys. Rev. B: Condens. Matter. 76 (2007) 205320.
[48] V. Coropceanu, J. Cornil, D.A. da Silva, Y. Olivier, R. Silbey, J.L. Bredas, Chem. Rev. 107 (2007) 926.
[49] M.D. Curtis, J. Cao, J.W. Kampf, J. Am. Chem. Soc. 126 (2004) 4318.
[50] F.J.M. Hoeben, P. Jonkheijm, E.W. Meijer, A.P.H.J. Schenning, Chem. Rev. 105 (2005) 1491.
[51] A.R. Murphy, J.M.J. Frechet, Chem. Rev. 107 (2007) 1066.
[52] S. Gunes, H. Neugebauer, N.S. Sariciftci, Chem. Rev. 107 (2007) 1324.
[53] Y.-J. Cheng, S.-H. Yang, C.-S. Hsu, Chem. Rev. 109 (2009) 5868.
[54] Z.H. Liu, J.H. Oh, M.E. Roberts, P. Wei, B.C. Paul, M. Okajima, Y. Nishi, Z.N. Bao, Appl. Phys. Lett. 94 (2009) 203301.

[55] H. Kusai, T. Nagano, K. Imai, Y. Kubozono, Y. Sako, Y. Takaguchi, A. Fujiwara, N. Akima, Y. Iwasa, S. Hino, Appl. Phys. Lett. 88 (2006) 173509.
[56] D.H. Kim, B.L. Lee, H. Moon, H.M. Kang, E.J. Jeong, J.I. Park, K.M. Han, S. Lee, B.W. Yoo, B.W. Koo, J.Y. Kim, W.H. Lee, K. Cho, H.A. Becerril, Z. Bao, J. Am. Chem. Soc. 131 (2009) 6124.
[57] D.K. Aswal, S. Lenfant, D. Guerin, J.V. Yakhmi, D. Vuillaume, Anal. Chim. Acta 568 (2006) 84.
[58] C. Celle, C. Suspene, J.P. Simonato, S. Lenfant, M. Ternisien, D. Vuillaume, Org. Electron. 10 (2009) 119.
[59] M. Mottaghi, P. Lang, F. Rodriguez, A. Rumyantseva, A. Yassar, G. Horowitz, S. Lenfant, D. Tondelier, D. Vuillaume, Adv. Funct. Mater. 17 (2007) 597.
[60] S.G.J. Mathijssen, E.C.P. Smits, P.A. van Hal, H.J. Wondergem, S.A. Ponomarenko, A. Moser, R. Resel, P.A. Bobbert, M. Kemerink, R.A.J. Janssen, D.M. de Leeuw, Nat. Nanotechnol. 4 (2009) 674.
[61] H. Yan, Z. Chen, Y. Zheng, C. Newman, J.R. Quinn, F. Dotz, M. Kastler, A. Facchetti, Nature 457 (2009) 679.
[62] Z. Chen, Y. Zheng, H. Yan, A. Facchetti, J. Am. Chem. Soc. 131 (2008) 8.
[63] A.L. Briseno, S.C.B. Mannsfeld, P.J. Shamberger, F.S. Ohuchi, Z.N. Bao, S.A. Jenekhe, Y.N. Xia, Chem. Mater. 20 (2008) 4712.
[64] D.W. Wang, Y. Bunimovich, A. Boukai, J.R. Heath, Small 3 (2007) 2043.
[65] Y.-Y. Noh, N. Zhao, M. Caironi, H. Sirringhaus, Nat. Nanotechnol. 2 (2007) 784.
[66] C.W. Sele, T. von Werne, R.H. Friend, H. Sirringhaus, Adv. Mater. 17 (2005) 997.
[67] C. Piliego, F. Cordella, D. Jarzab, S. Lu, Z. Chen, A. Facchetti, M.A. Loi, Appl. Phys. A: Mater. Sci. Process. 95 (2009) 303.
[68] Y.N. Gao, P. Ma, Y.L. Chen, Y. Zhang, Y.Z. Bian, X.Y. Li, J.Z. Jiang, C.Q. Ma, Inorg. Chem. 48 (2009) 45.
[69] P. Jonkheijm, N. Stutzmann, Z.J. Chen, D.M. de Leeuw, E.W. Meijer, A. Schenning, F. Würthner, J. Am. Chem. Soc. 128 (2006) 9535.
[70] H.L. Yip, H. Ma, A.K.Y. Jen, J.C. Dong, B.A. Parviz, J. Am. Chem. Soc. 128 (2006) 5672.
[71] W. Kim, A. Javey, O. Vermesh, O. Wang, Y.M. Li, H.J. Dai, Nano Lett. 3 (2003) 193.
[72] G. Robert, V. Derycke, M.F. Goffman, S. Lenfant, D. Vuillaume, J.P. Bourgoin, Appl. Phys. Lett. 93 (2008) 143117.
[73] S.A. DiBenedetto, D. Frattarelli, M.A. Ratner, A. Facchetti, T.J. Marks, J. Am. Chem. Soc. 130 (2008) 7528.
[74] S.A. DiBenedetto, D.L. Frattarelli, A. Facchetti, M.A. Ratner, T.J. Marks, J. Am. Chem. Soc. 131 (2009) 11080.
[75] B. Singh, N.S. Sariciftci, J.G. Grote, F.K. Hopkins, J. Appl. Phys. 100 (2006) 024514.
[76] P. Stadler, K. Oppelt, T.B. Singh, J.G. Grote, R. Schwodiauer, S. Bauer, H. Piglmayer-Brezina, D. Bauerle, N.S. Sariciftci, Org. Electron. 8 (2007) 648.
[77] K.C. See, A. Becknell, J. Miragliotta, H.E. Katz, Adv. Mater. 19 (2007) 3322.
[78] L. Torsi, A. Dodabalapur, L. Sabbatini, P.G. Zambonin, Sens. Actuators B: Chem. 67 (2000) 312.
[79] G.F. Cerofolini, G. Arena, M. Camalleri, C. Galati, S. Reina, L. Renna, D. Mascolo, V. Nosik, Microelectron. Eng. 81 (2005) 405.
[80] Z.N. Bao, L. Chen, M. Weldon, E. Chandross, O. Cherniavskaya, Y. Dai, J.B.H. Tok, Chem. Mater. 14 (2002) 24.
[81] R. Martins, P. Barquinha, L. Pereira, N. Correia, G. Goncalves, I. Ferreira, E. Fortunato, Appl. Phys. Lett. 93 (2008) 203501.
[82] A.J. Heeger, Solid State Commun. 107 (1998) 673.
[83] See, for example: http://kodak.com/US/en/corp/display/index.jhtml; http://www.research.philips.com/; http://www.dupont.com/displays/oled/; http://www.cdtltd.co.uk/; http://www.universaldisplay.com/.
[84] A.P. Kulkarni, C.J. Tonzola, A. Babel, S.A. Jenekhe, Chem. Mater. 16 (2004) 4556.
[85] R.H. Friend, R.W. Gymer, A.B. Holmes, J.H. Burroughes, R.N. Marks, C. Taliani, D.D.C. Bradley, D.A.D. Santos, J.L. Brédas, M. Lögdlund, W.R. Salaneck, Nature 397 (1999) 121.
[86] J. Cui, Q. Huang, Q. Wang, T.J. Marks, Langmuir 17 (2001) 2051.
[87] L.S. Hung, C.H. Chen, Mater. Sci. Eng. R 39 (2002) 143.
[88] R.U.A. Khan, O.-P. Kwon, A. Tapponnier, A.N. Rashid, P. Günter, Adv. Funct. Mater. 16 (2006) 180.
[89] R. Jagannathan, G. Irvin, T. Blanton, S. Jagannathan, Adv. Funct. Mater. 16 (2006) 747.
[90] S.-C. Chang, J. Bharathan, Y. Yang, R. Helgeson, F. Wudl, M.B. Ramey, J.R. Reynolds, Appl. Phys. Lett. 73 (1998) 2561.
[91] S.-C. Chang, J. Liu, J. Bharathan, Y. Yang, J. Onohara, J. Kido, Adv. Mater. 11 (1999) 734.
[92] Y. Yang, S.-C. Chang, J. Bharathan, J. Liu, J. Mater. Sci.: Mater. Electron. 11 (2000) 89.
[93] J. Ouyang, T.-F. Guo, Y. Yang, H. Higuchi, M. Yoshioka, T. Nagatsuka, Adv. Mater. 14 (2002) 915.
[94] K. Tada, M. Onoda, Thin Solid Films 438–439 (2003) 365.
[95] R. Advincula, C. Xia, K. Onishi, A. Baba, W. Knoll, Polym. Prep. (Am. Chem. Soc., Div. Polym. Chem.) 44 (2003) 309.
[96] D.A. Pardo, G.E. Jabbour, N. Peyghambarian, Adv. Mater. 12 (2000) 1249.
[97] J. Birnstock, J. Blassing, A. Hunze, M. Scheffel, M. Stossel, K. Heuser, G. Wittmann, J. Worle, A. Winnacker, Appl. Phys. Lett. 78 (2001) 3905.
[98] J. Birnstock, J. Blässing, A. Hunze, M. Scheffel, M. Stössel, K. Heuser, J. Wörle, G. Wittmann, A. Winnacker, Proc. SPIEs Int. Soc. Opt. Eng. 4464 (2002) 68.
[99] K. Tada, M. Onoda, Thin Solid Films 499 (2006) 19.
[100] S.-R. Tseng, S.-C. Lin, H.-F. Meng, H.-H. Liao, C.-H. Yeh, H.-C. Lai, S.-F. Horng, C.-S. Hsu, Appl. Phys. Lett. 88 (2006), 163501/1.
[101] J. Carter, A. Wehrum, M.C. Dowling, M. Cacheiro-Martinez, N.D.B. Baynes, Proc. SPIEs Int. Soc. Opt. Eng. 4800 (2003) 34.
[102] J. Steiger, S. Heun, N.J. Tallant, Imaging Sci. Technol. 47 (2003) 473.
[103] Z. Zhu, T.M. Swager, J. Am. Chem. Soc. 124 (2002) 9670.
[104] C.I. Wilkinson, D.G. Lidzey, L.C. Palilis, R.B. Fletcher, S.J. Martin, X.H. Wang, D.D.C. Bradley, Appl. Phys. Lett. 79 (2001) 171.
[105] F.A. Boroumand, P.W. Fry, G.G. Lidzey, Nano Lett. 5 (2005) 67.
[106] A.C. Grimsdale, K.L. Chan, R.E. Martin, P.G. Jokisz, A.B. Holmes, Chem. Rev. 109 (2009) 897.
[107] G. Decher, Science 277 (1997) 1232.
[108] G. Decher, J.B. Schlenoff (Eds.), Multilayer Thin Films, Wiley, Weinheim, 2003.
[109] P.T. Hammond, Curr. Opin. Colloid Interface Sci. 4 (2000) 430.
[110] M. Schonhoff, Curr. Opin. Colloid Interface Sci. 8 (2003) 86.
[111] G. Decher, J.D. Hong, J. Schmitt, Thin Solid Films 210 (1992) 831.
[112] J. Stepp, J.B. Schlenoff, J. Electrochem. Soc. 144 (1997) L155.
[113] D.M. DeLongchamp, M. Kastantin, P.T. Hammond, Chem. Mater. 15 (2003) 1575.
[114] D.M. DeLongchamp, P.T. Hammond, Chem. Mater. 16 (2004) 4799.
[115] D.M. DeLongchamp, P.T. Hammond, Adv. Funct. Mater. 14 (2004) 224.
[116] D.G. Kurth, D. Volkmer, M. Ruttorf, B. Richter, A. Müller, Chem. Mater. 12 (2000) 2829.
[117] F. Caruso, D.G. Kurth, D. Volkmer, M.J. Koop, A. Müller, Langmuir 14 (1998) 3462.
[118] S.Q. Liu, H. Mohwald, D. Volkmer, D.G. Kurth, Langmuir 22 (2006) 1949.
[119] F. Arnaud-Neu, M.-J. Schwing-Weill, Bull. Soc. Chim. Fr. (1973) 3225.
[120] T. Yamase, M.J. Suga, J. Chem. Soc., Dalton Trans. 4 (1989) 661.
[121] T. Yamase, P. Prokop, Y. Arai, J. Mol. Struct. 656 (2003) 107.
[122] H. Hong, R. Sfez, E. Vaganova, S. Yitzchaik, D. Davidov, Thin Solid Films 366 (2000) 260.
[123] M. Elhabiri, A.M. Albrecht-Gary, Coord. Chem. Rev. 252 (2008) 1079.
[124] S.-C. Yu, C.-C. Kwok, W.-K. Chan, C.-M. Che, Adv. Mater. 15 (2003) 1643.
[125] M. Higuchi, Polym. J. 41 (2009) 511.
[126] C. Legnani, R. Reyes, M. Cremon, I.A. Bagatin, H.E. Toma, Appl. Phys. Lett. 85 (2004) 10.
[127] H.C. Lin, C.M. Tsai, G.H. Huang, Y.T. Tao, Macromolecules 39 (2006) 557.
[128] P.L. Huyskens, W.A.P. Luck, Intermolecular Forces, 3d ed., Springer-Verlag, Berlin, 1991.
[129] C.A. Hunter, H.L. Anderson, Angew. Chem. Int. Ed. 48 (2009) 7488.
[130] P.J. Yang, C.W. Wu, D. Sahu, H.C. Lin, Macromolecules 41 (2008) 9692.
[131] Y.Z.J. Luo, Z.-Q. Niu, Q.-F. Zhou, Y. Ma, J. Pei, J. Am. Chem. Soc. 129 (2007) 11314.
[132] C.-C. Wu, T.-L. Liu, W.-Y. Hung, Y.-T. Lin, K.-T. Wong, R.-T. Chen, Y.-M. Chen, Y.-Y. Chien, J. Am. Chem. Soc. 125 (2003) 3710.
[133] K.-T. Wong, Y.-L. Liao, Y.-T. Lin, H.-C. Su, C.-C. Wu, Org. Lett. 7 (2005) 5131.
[134] T.P.I. Saragi, T. Spehr, A. Siebert, T. Fuhrmann-Lieker, J. Salbeck, Chem. Rev. 107 (2007) 1011.
[135] J. Luo, T. Lei, X. Xu, F.-M. Li, Y. Ma, K. Wu, J. Pei, Chem. Eur. J. 14 (2008) 3860.
[136] S.P. Dudek, M. Pouderoijen, R. Abbel, A.P.H.J. Schenning, E.W. Meijer, J. Am. Chem. Soc. 127 (2005) 11763.
[137] A.N. Rashid, C. Erny, P. Günter, Adv. Mater. 15 (2003) 2024.
[138] N.R. Armstrong, R.M. Wightman, E.M. Gross, Annu. Rev. Phys. Chem. 52 (2001) 391.
[139] D. Neher, J. Grüner, V. Cimrová, W. Schmidt, R. Rulkens, U. Lauter, Polym. Adv. Technol. 9 (1998) 461.
[140] Q. Pei, Y. Yang, J. Am. Chem. Soc. 118 (1996) 7416.
[141] Q. Pei, Y. Yang, G. Yu, C. Zhang, A.J. Heeger, J. Am. Chem. Soc. 118 (1996) 3922.
[142] Q. Pei, G. Yu, C. Zhang, Y. Yang, A.J. Heeger, Science 269 (1995) 1086.
[143] G. Yu, Synth. Met. 80 (1996) 143.
[144] S. Becker, C. Ego, A.C. Grimsdale, E.J.W. List, D. Marsitzky, A. Pogantsch, S. Setayesh, G. Leising, K. Müllen, Synth. Met. 125 (2001) 73.
[145] B.S. Chuah, D.-H. Hwang, S.T. Kim, S.C. Moratti, A.B. Holmes, J.C. de Mello, R.H. Friend, Synth. Met. 91 (1997) 279.
[146] L. Holzer, B. Winkler, F.P. Wenzl, S. Tasch, L. Dai, A.W.H. Mau, G. Leising, Synth. Met. 100 (1999) 71.
[147] D.H. Hwang, B.S. Chuah, X.C. Li, S.T. Kim, S.C. Moratti, A.B. Holmes, J.C. de Mello, R.H. Friend, Macromol. Symp. 125 (1997) 111.
[148] C. Huang, W. Huang, J. Guo, C.-Z. Yang, Polym. Prep. (Am. Chem. Soc., Div. Polym. Chem.) 41 (2000) 1271.
[149] F. Kong, S.Y. Zhang, J.K. Shen, Y. Zheng, C.G. Ou, C.Z. Yang, X.L. Wu, X.M. Bao, R.K. Yuan, Synth. Met. 137 (2003) 1083.
[150] B.S. Chuah, F. Geneste, A.B. Holmes, R.E. Martin, H. Rost, F. Cacialli, R.H. Friend, H. Hörhold, S. Pfeiffer, D.-H. Hwang, Macromol. Symp. 154 (2000) 177.
[151] A.B. Holmes, B.S. Chuah, X.-C. Li, F. Cacialli, J. Morgado, H. Sirringhaus, D.A. dos Santos, S.C. Moratti, J.-L. Brédas, R.H. Friend, F. Garnier, Proc. SPIEs Int. Soc. Opt. Eng. 3476 (1998) 24.
[152] J. Morgado, F. Cacialli, R.H. Friend, B.S. Chuah, S.C. Moratti, A.B. Holmes, Synth. Met. 111–112 (2000) 449.
[153] T.-W. Lee, H.-C. Lee, O.O. Park, Appl. Phys. Lett. 81 (2002) 214.
[154] B.S. Chuah, D.-H. Hwang, S.M. Chang, J.E. Davies, S.C. Moratti, X.-C. Li, A.B. Holmes, J.C. de Mello, N. Tessler, R.H. Friend, Proc. SPIEs Int. Soc. Opt. Eng. 3148 (1997) 132.
[155] J. Morgado, F. Cacialli, R.H. Friend, B.S. Chuah, H. Rost, A.B. Holmes, Macromolecules 34 (2001) 3094.
[156] J. Morgado, F. Cacialli, R.H. Friend, B.S. Chuah, H. Rost, S.C. Moratti, A.B. Holmes, Synth. Met. 119 (2001) 595.

[157] H. Rost, B.S. Chuah, D.H. Hwang, S.C. Moratti, A.B. Holmes, J. Wilson, J. Morgado, J.J.M. Halls, J.C. de Mello, R.H. Friend, Synth. Met. 102 (1999) 937.
[158] T. Johansson, W. Mammo, M.R. Andersson, O. Inganäs, Chem. Mater. 11 (1999) 3133.
[159] Q. Sun, H. Wang, C. Yang, G. He, Y. Li, Synth. Met. 128 (2002) 161.
[160] Q. Sun, H. Wang, C. Yang, Y. Li, J. Mater. Chem. 13 (2003) 800.
[161] Q. Sun, H. Wang, C. Yang, Y. Li, Synth. Met. 137 (2003) 1087.
[162] H. Wang, X. Wang, D. Liu, Synth. Met. 126 (2002) 219.
[163] Q. Sun, C. Yang, J. Zhai, L. Jiang, Y. Li, H. Wang, Synth. Met. 137 (2003) 1089.
[164] J.S. Wilson, M.J. Frampton, J.J. Michels, L. Sardone, G. Marletta, R.H. Friend, P. Samori, H.L. Anderson, F. Cacialli, Adv. Mater. 17 (2005) 2659.
[165] H.J. Bolink, L. Cappelli, E. Coronado, M. Gratzel, M.K. Nazeeruddin, J. Am. Chem. Soc. 128 (2006) 46.
[166] S. Graber, K. Doyle, M. Neuburger, C.E. Housecroft, E.C. Constable, R.D. Costa, E. Orti, D. Repetto, H.J. Bolink, J. Am. Chem. Soc. 130 (2008) 14944.
[167] N. Armaroli, G. Accorsi, F. Cardinali, A. Listorti, Top. Curr. Chem. 280 (2007) 69.
[168] A. Petrella, M. Tamborra, P. Cosma, M.L. Curli, M. Striccoli, R. Comparelli, A. Agostiano, Thin Solid Films 516 (2008) 5010.
[169] H. Hoppe, N.S. Sariciftci, J. Mater. Res. 19 (2004) 1924.
[170] J. Roncali, P. Leriche, A. Cravino, Adv. Mater. 19 (2007) 2045.
[171] M. Campoy-Quiles, T. Ferenczi, T. Agostinelli, P.G. Etchegoin, Y. Kim, T.D. Anthopoulos, P.N. Stavrinou, D.D.C. Bradley, J. Nelson, Nat. Mater. 7 (2008) 158.
[172] J.-L. Brédas, J.E. Norton, J. Cornil, V. Coropceanu, Acc. Chem. Res. 42 (2009) 1691.
[173] G. Yu, J. Gao, J.C. Hummelen, F. Wudl, A.J. Heeger, Science 270 (1995) 1789.
[174] Solarmer Energy, Inc. reported an efficiency of 7.9% for OPV devices with a 0.1 cm^2 active area. Source: www.Solarmer.com.
[175] J. Peet, A.J. Heeger, G.C. Bazan, Acc. Chem. Res. 42 (2009) 1700.
[176] S.E. Shaheen, C.J. Brabec, N.S. Sariciftci, F. Padinger, T. Fromherz, J.C. Hummelen, Appl. Phys. Lett. 78 (2001) 841.
[177] J.J.M. Halls, K. Pichler, R.H. Friend, S.C. Moratti, A.B. Holmes, Appl. Phys. Lett. 68 (1996) 3120.
[178] E.H.A. Beckers, Z.J. Chen, S.C.J. Meskers, P. Jonkheijm, A. Schenning, X.Q. Li, P. Osswald, F. Wurthner, R.A.J. Janssen, J. Phys. Chem. B 110 (2006) 16967.
[179] J.E. Bullock, R. Carmieli, S.M. Mickley, J. Vura-Weis, M.R. Wasielewski, J. Am. Chem. Soc. 131 (2009) 11919.
[180] J. Li, M. Kastler, W. Pisula, J.W.F. Robertson, D. Wasserfallen, A.C. Grimsdale, J. Wu, K. Müllen, Adv. Funct. Mater. 17 (2007) 2528.
[181] M. Linke-Schaetzel, A.D. Bhise, H. Gliemann, T. Koch, T. Schimmel, T.S. Balaban, Thin Solid Films 451 (2004) 16.
[182] T.S. Balaban, Acc. Chem. Res. 38 (2005) 612.
[183] O.K. Kim, J. Melinger, S.J. Chung, M. Pepitonet, Org. Lett. 10 (2008) 1625.
[184] E. Charlet, E. Grelet, P. Brettes, H. Bock, H. Saadaoui, L. Cisse, P. Destruel, N. Gherardi, I. Seguy, Appl. Phys. Lett. 92 (2008).
[185] S. Archambeau, I. Seguy, P. Jolinat, J. Farenc, P. Destruel, T.P. Nguyen, H. Bock, E. Grelet, Appl. Surf. Sci. 253 (2006) 2078.
[186] R.D. Kennedy, A.L. Ayzner, D.D. Wanger, C.T. Day, M. Halim, S.I. Khan, S.H. Tolbert, B.J. Schwartz, Y. Rubin, J. Am. Chem. Soc. 130 (2008) 17290.
[187] A.L. Sisson, N. Sakai, N. Banerji, A. Furstenberg, E. Vauthey, S. Matile, Angew. Chem. Int. Ed. 47 (2008) 3727.
[188] N. Sakai, A.L. Sisson, T. Burgi, S. Matile, J. Am. Chem. Soc. 129 (2007) 15758.
[189] R. Bhosale, J. Misek, N. Sakai, S. Matile, Chem. Soc. Rev. 39 (2010) 138.
[190] A. Mishra, C.Q. Ma, P. Bauerle, Chem. Rev. 109 (2009) 1141.
[191] F. Würthner, Z. Chen, F.J.M. Hoeben, P. Osswald, C.-C. You, P. Jonkheijm, J. von Herrikhuyzen, A.P.H.J. Schenning, P.P.A.M. van der Schoot, E.W. Meijer, E.H.A. Beckers, S.C.J. Meskers, R.A.J. Janssen, J. Am. Chem. Soc. 126 (2004) 10611.
[192] L. Sanchez, N. Martin, D.M. Guldi, Angew. Chem. Int. Ed. 44 (2005) 5374.
[193] M. Fourmigue, P. Batail, Chem. Rev. 104 (2004) 5379.
[194] Y. Kobayashi, M. Yoshioka, K. Saigo, D. Hashizume, T. Ogura, J. Am. Chem. Soc. 131 (2009) 9995.
[195] C.H. Huang, N.D. McClenaghan, A. Kuhn, J.W. Hofstraat, D.M. Bassani, Org. Lett. 7 (2005) 3409.
[196] C.H. Huang, N.D. McClenaghan, A. Kuhn, G. Bravic, D.M. Bassani, Tetrahedron 62 (2006) 2050.
[197] N.D. McClenaghan, Z. Grote, K. Darriet, M. Zimine, R.M. Williams, L. De Cola, D.M. Bassani, Org. Lett. 7 (2005) 807.
[198] C.Y. Jiang, P. Liu, W.J. Deng, Synth. Commun. 39 (2009) 2360.
[199] R. Mezzenga, J. Ruokolainen, G.H. Fredrickson, E.J. Kramer, D. Moses, A.J. Heeger, O. Ikkala, Science 299 (2003) 1872.
[200] M. Lee, B.K. Cho, W.C. Zin, Chem. Rev. 101 (2001) 3869.
[201] S. Barrau, T. Heiser, F. Richard, C. Brochon, C. Ngov, K. van de Wetering, G. Hadziioannou, D.V. Anokhin, D.A. Ivanov, Macromolecules 41 (2008) 2701.
[202] N. Sary, L. Rubatat, C. Brochon, G. Hadziioannou, R. Mezzenga, Macromol. Symp. 268 (2008) 28.
[203] R.A. Segalman, B. McCulloch, S. Kirmayer, J.J. Urban, Macromolecules 42 (2009) 9205.
[204] A. Laiho, R.H.A. Ras, S. Valkama, J. Ruokolainen, R. Osterbacka, O. Ikkala, Macromolecules 39 (2006) 7648.
[205] M.W. Rowell, M.A. Topinka, M.D. McGehee, H.J. Prall, G. Dennler, N.S. Sariciftci, L.B. Hu, G. Gruner, Appl. Phys. Lett. 88 (2006) 3.
[206] G.M.A. Rahman, D.M. Guldi, R. Cagnoli, A. Mucci, L. Schenetti, L. Vaccari, M. Prato, J. Am. Chem. Soc. 127 (2005) 10051.
[207] A.F. Nogueira, B.S. Lomba, M.A. Soto-Oviedo, C.R.D. Correia, P. Corio, C.A. Furtado, I.A. Hummelgen, J. Phys. Chem. C 111 (2007) 18431.
[208] E. Kymakis, I. Alexandrou, G.A.J. Amaratunga, J. Appl. Phys. 93 (2003) 1764.
[209] E. Kymakis, G.A.J. Amaratunga, Appl. Phys. Lett. 80 (2002) 112.
[210] H. Ago, K. Petritsch, M.S.P. Shaffer, A.H. Windle, R.H. Friend, Adv. Mater. 11 (1999) 1281.
[211] S. Berson, R. de Bettignies, S. Bailly, S. Guillerez, B. Jousselme, Adv. Funct. Mater. 17 (2007) 3363.
[212] D.A. Britz, A.N. Khlobystov, Chem. Soc. Rev. 35 (2006) 637.
[213] D.M. Guldi, G.M.A. Rahman, N. Jux, N. Tagmatarchis, M. Prato, Angew. Chem. Int. Ed. 43 (2004) 5526.
[214] J.E. Klare, I.P. Murray, J. Goldberger, S.I. Stupp, Chem. Commun. (2009) 3705.
[215] S.C. Kang, T. Umeyama, M. Ueda, Y. Matano, H. Hotta, K. Yoshida, S. Isoda, M. Shiro, H. Imahori, Adv. Mater. 18 (2006) 2549.
[216] H. Imahori, A. Fujimoto, S. Kang, H. Hotta, K. Yoshida, T. Umeyama, Y. Matano, S. Isoda, M. Isosomppi, N.V. Tkachenko, H. Lemmetyinen, Chem. Eur. J. 11 (2005) 7265.
[217] R. Baron, C.H. Huang, D.M. Bassani, A. Onopriyenko, M. Zayats, I. Willner, Angew. Chem. Int. Ed. 44 (2005) 4010.
[218] G. Calzaferri, S. Huber, H. Maas, C. Minkowski, Angew. Chem. Int. Ed. 42 (2003) 3732.
[219] G. Calzaferri, H.R. Li, D. Bruhwiler, Chem. Eur. J. 14 (2008) 7442.
[220] R. Koeppe, O. Bossart, G. Calzaferri, N.S. Sariciftci, Sol. Energy Mater. Sol. Cells 91 (2007) 986.
[221] B. Oregan, M. Grätzel, Nature 353 (1991) 737.
[222] U. Bach, D. Lupo, P. Comte, J.E. Moser, F. Weissortel, J. Salbeck, H. Spreitzer, M. Grätzel, Nature 395 (1998) 583.
[223] M. Grätzel, Nature 414 (2001) 338.
[224] M. Grätzel, Acc. Chem. Res. 42 (2009) 1788.
[225] B.E. Hardin, E.T. Hoke, P.B. Armstrong, J.H. Yum, P. Comte, T. Torres, J.M.J. Frechet, M.K. Nazeeruddin, M. Gratzel, M.D. McGehee, Nat. Photon 3 (2009) 406.
[226] S. Handa, H. Wietasch, M. Thelakkat, J.R. Durrant, S.A. Haque, Chem. Commun. (2007) 1725.
[227] R. Argazzi, N.Y.M. Iha, H. Zabri, F. Odobel, C.A. Bignozzi, Coord. Chem. Rev. 248 (2004) 1299.
[228] Y.J. Kim, J.H. Kim, M.S. Kang, M.J. Lee, J. Won, J.C. Lee, Y.S. Kang, Adv. Mater. 16 (2004) 1753.
[229] N. Hirata, J.J. Lagref, E.J. Palomares, J.R. Durrant, M.K. Nazeeruddin, M. Gratzel, D. Di Censo, Chem. Eur. J. 10 (2004) 595.
[230] C. Martini, G. Poize, D. Ferry, D. Kanehira, N. Yoshimoto, J. Ackermann, F. Fages, ChemPhysChem 10 (2009) 2465.
[231] H. Imahori, J.C. Liu, H. Hotta, A. Kira, T. Umeyama, Y. Matano, G.F. Li, S. Ye, M. Isosomppi, N.V. Tkachenko, H. Lemmetyinen, J. Phys. Chem. B 109 (2005) 18465.
[232] F.M. Raymo, Adv. Mater. 14 (2002) 401.
[233] B.L. Feringa (Ed.), Molecular Switches, Wiley–VCH, Weinheim, 2001.
[234] A.P. de Silva, N.H.Q. Gunaratne, C.P. McCoy, Nature 364 (1993) 42.
[235] J. Andréasson, U. Pischel, Chem. Soc. Rev. 39 (2010) 174.
[236] K. Szaciłowski, Chem. Rev. 108 (2008) 3481.
[237] V. Balzani, M. Venturi, A. Credi, Molecular Devices and Machines, Wiley–VCH, Weinheim, 2008.
[238] A.P. de Silva, N.D. McClenaghan, Chem. Eur. J. 10 (2004) 574.
[239] T. Gupta, M.E.v.d. Boom, Angew. Chem. Int. Ed. 47 (2008) 5322.
[240] N.G. Portney, R.J. Tseng, G. Destito, E. Strable, Y. Yang, M. Manchester, M.G. Finn, M. Ozkan, Appl. Phys. Lett. 90 (2007) 214104.
[241] J.J. Davis, G.A. Orlowski, H. Rahman, P.D. Beer, Chem. Commun. 46 (2010) 54.
[242] V. Balzani, A. Credi, M. Venturi, ChemPhysChem 9 (2008) 1.
[243] J. Berna, D.A. Leigh, M. Lubomska, S.M. Mendoza, E.M. Perez, P. Rudolf, G. Teobaldi, F. Zerbetto, Nature Mater. 4 (2005) 704.
[244] N. Wintjes, D. Bonifazi, F. Cheng, A. Kiebele, M. Stöhr, T. Jung, H. Spillmann, F. Diederich, Angew. Chem. Int. Ed. 46 (2007) 4089.
[245] L.X. Mu, W.S. Shi, G.W. She, J.C. Chang, S.T. Lee, Angew. Chem. Int. Ed. 48 (2009) 3469.
[246] A.P. de Silva, M.R. James, B.O.F. McKinney, D.A. Pears, S.M. Weir, Nat. Mater. 5 (2006) 787.
[247] R. Klajn, L. Fang, A. Coskun, M.A. Olson, P.J. Wesson, J.F. Stoddart, B.A. Grzybowski, J. Am. Chem. Soc. 131 (2009) 4233.
[248] S. Malkmus, F.O. Koller, S. Draxler, T.E. Schrader, W.J. Schreier, T. Brust, J.A. DiGirolamo, W.J. Lees, W. Zinth, M. Braun, Adv. Funct. Mater. 17 (2007) 3657.
[249] M. Irie, T. Fukaminato, T. Sasaki, N. Tamai, T. Kawai, Nature 420 (2002) 759.
[250] J. Andréasson, S.D. Straight, S. Bandyopadhyay, R.H. Mitchell, T.A. Moore, A.L. Moore, D. Gust, Angew. Chem. Int. Ed. 46 (2007) 958.
[251] C.P. Collier, G. Mattersteig, E.W. Wong, Y. Luo, K. Beverly, J. Sampaio, F.M. Raymo, J.F. Stoddart, J.R. Heath, Science 289 (2000) 1172.
[252] J.E. Green, J.W. Choi, A. Boukai1, Y. Bunimovich, E. Johnston-Halperin, E. DeIonno, Y. Luo, B.A. Sheriff, K. Xu, Y.S. Shin, H.-R. Tseng, J.F. Stoddart, J.R. Heath, Nature 445 (2007) 414.